COMPARING THE MECHANICAL PROPERTIES OF SHALE CORES:

INTACT VS. FRACTURED AND SEALED WITH UICP

by

Kayla Marjorie Bedey

A thesis submitted in partial fulfillment
of the requirements for the degree

of

Master of Science

in

Environmental Engineering

MONTANA STATE UNIVERSITY
Bozeman, Montana

December 2023

ACKNOWLEDGEMENTS

Thank you to my graduate committee, Dr. Adrienne Phillips, Dr. Catherine Kirkland, and Dr. Kirsten Matteson. Their guidance, motivations, opportunities, and support allowed me to flourish and complete this work. Special thanks to my research partner, Matthew Willett, for his kind and diligent nature. I am especially grateful to Al Cunningham for guiding and helping me along the way. My gratitude goes to the people and resources in the Center for Biofilm Engineering and the Civil Engineering Department. I would also like to thank Ladean McKittrick for training me on equipment that made this project possible and Joe Eldring for helping me design a testing fixture that allowed this project to take shape. This project was made possible through funding from the Department of Energy, Office of Basic Earth Sciences (DOE Award No.: DE-SC0021324), with a shoutout to Dr. Dustin Crandall at the National Energy Technology Laboratory in Morgantown, West Virginia. Huge thanks to my family and friends for their support and understanding. Finally, I am forever thankful to my husband, Sam Lowe, and our cat, Dingus, for their endless love and support.

TABLE OF CONTENTS

LIST OF TABLES

Table Page

LIST OF FIGURES

Figure Page

LIST OF FIGURES CONTINUED

Figure Page

LIST OF FIGURES CONTINUED

Figure Page

LIST OF FIGURES CONTINUED

Figure Page

ABSTRACT

Fractures in subsurface shale formations are instrumental in the recovery of hydrocarbon resources. A result of hydraulic fracturing, these fractures have the potential to become harmful leakage pathways that may contribute undesired fluids to the atmosphere and functional groundwater aquifers. Ureolysis-induced calcium carbonate precipitation (UICP) is a biomineral solution where the urease enzyme converts urea and calcium into calcium carbonate mineral. The resulting biomineral can bridge gaps in fractured shale, reduce undesired fluid flow through leakage pathways, limit fracture propagation, better store carbon dioxide, and potentially extend the efficiency of future and existing wells. The mechanical properties of fractured shale sealed with UICP was investigated using a modified Brazilian indirect tensile strength test. Part one of this study investigated the tensile strength of shale rock using intact Eagle Ford (EF) and Wolfcamp (WC) shale cores (5.08 cm long by 2.54 cm diameter) tested at room temperature (RT) and 60°C. Results show no significant difference between shale types (average tensile strength = 6.19 MPa). EF cores displayed a higher strength at RT versus 60°C, but no difference was seen between temperatures for WC cores. Part two used UICP to seal shale cores (5.08 cm long by 2.54 cm diameter) with a single, heterogeneous fracture spanning the core length. UICP was delivered two ways: 1) the flow-through method injected 20-30 sequential patterns of microbes and UICP-promoting fluids into the fracture until fracture permeability reduced by three orders of magnitude and 2) the immersion method placed cores treated with guar gum and UICP-promoting solutions into a batch reactor, demonstrating that guar gum is a suitable inclusion to UICP-technology and may be capable of reducing the number of injections required in flow-through methodology. Tensile results for both flow-through and immersion methods were widely variable (0.15 – 8 MPa), and in some cores the biomineralized fracture split apart. Notably in other cores the biomineralized fracture remained intact, demonstrating more cohesion than the surrounding shale, indicating that UICP may produce a strong seal for subsurface application.

INTRODUCTION AND BACKGROUND

Motivations

Hydraulic Fracturing

Hydraulic fracturing, aka "fracking," is a popular subsurface reservoir stimulation technique used to extract hydrocarbon energy resources. Natural gas (i.e., shale gas) trapped within subsurface shale rock formations is a crucial energy source as the world transitions to more climate friendly and economically feasible alternatives. Shale formations, considered unconventional reservoirs, are characterized by low to ultra-low permeability that require stimulation to recover trapped resources due to hydrocarbon viscosity and reservoir matrix permeability (Peters et al., 2016). Stimulation involves injecting fracking fluids, comprised of water, proppant (sand), and proprietary chemicals, at high pressures down the wellbore creating an artificially induced fracture network, allowing accessible hydrocarbons to flow to the surface (Figure 1.1). Additionally, horizontal drilling expands the contact area between wellbore and reservoir, increasing hydrocarbon production per well. Economically, this revolutionary technology has stimulated energy independence, lowered fuel prices, and promoted job creation in the United States (Q. Wang et al., 2014). Consequently, hydraulic fracturing has been accused of contributing negative environmental impacts, such as groundwater aquifer contamination (Myers, 2012; Rodriguez et al., 2020; Vengosh et al., 2014), making it a highly controversial technology.

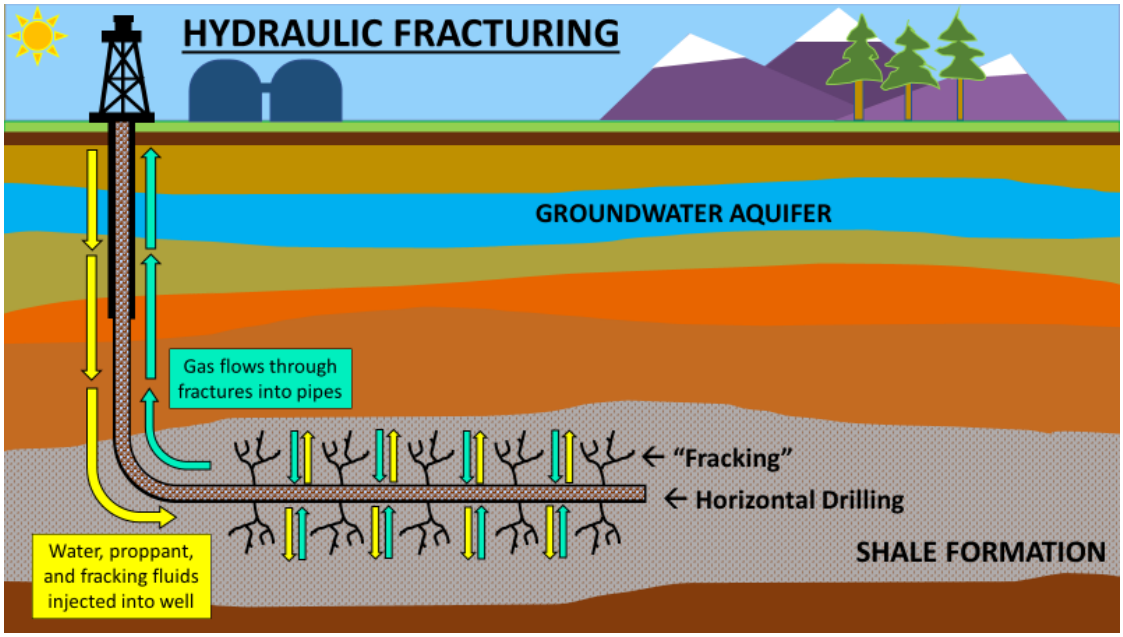

Figure 1.1. Hydraulic fracturing and horizontal drilling schematic.

Shale Rock

Shale is a fine-grained, sedimentary rock characterized by low permeability, an anisotropic nature, and finely bedded material that readily splits into thin layers, or laminations. Shale formations, also referred to as basins, are scattered throughout the United States. Shale plays are the regions within a basin that are currently fracked or prospectively frackable. Figure 1.2 highlights the distribution of major shale resources in the lower 48 states (U.S.E.I.A., 2016). Found at varying subsurface depths and thermal conditions, shale formations come in a variety of lithology and mineralogy, making some formations more conducive to hydraulic fracturing than others (Peters et al., 2016; Scotchman, 2016).

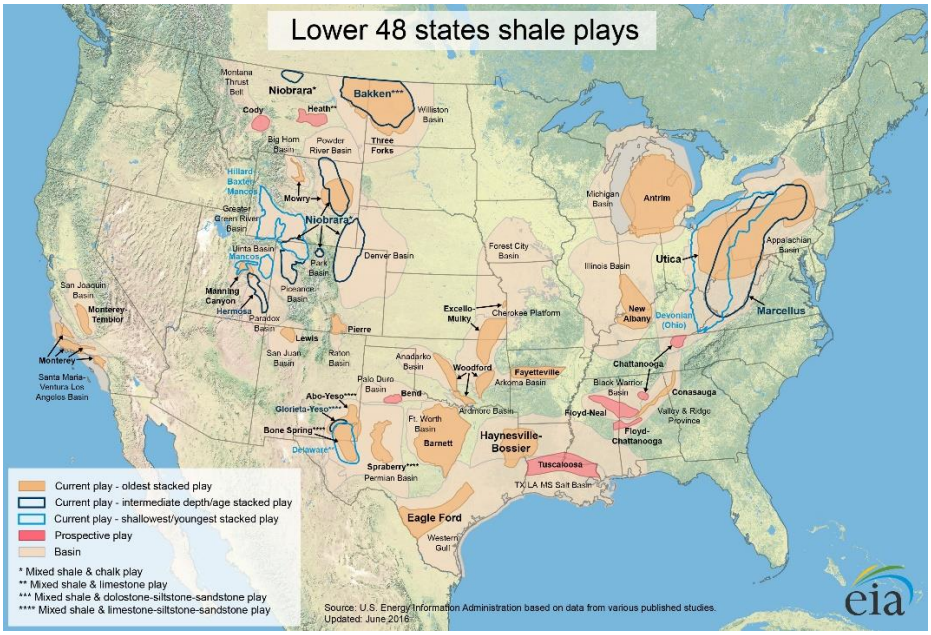

Figure 1.2. U.S. Energy Information Administration map of the distribution of major U.S. shale resources.

Shale brittleness is key to hydraulic fracturing success. Shale formations can be divided into four classifications based on lithology: silicate dominant, carbonate dominant, clay dominant, and strongly heterogenous, meaning they are not primarily dominant in either carbonates, silicates, or clay (Figure 1.3) (Mews et al., 2019). Shales containing a higher ratio of brittle minerals (e.g., silicates or carbonates) to ductile clays are the best candidates for hydraulic fracturing. Brittle shales more readily promote perforation and fracture initiation that form complex fracture networks, whereas ductile shales exhibit resistance to fracture growth and failure.

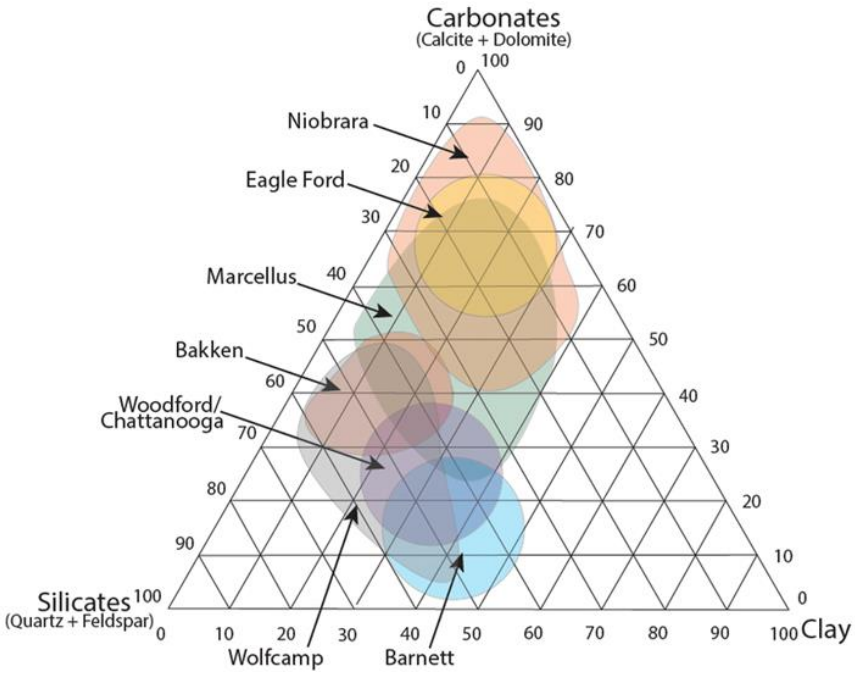

Figure 1.3. Ternary diagram presented by Mews et al. (2019) showing average mineral content for major US shale formations including: Niobrara, Eagle Ford, Marcellus, Bakken, Woodford/Chattanooga, Wolfcamp, and Barnett formations.

Why Seal Fractured Shale?

Fracture sealing in subsurface shale offers many incentives including offsetting potential environmental effects, better carbon dioxide storage, and enhanced hydrocarbon recovery. Fracking is controversial for creating potential contaminant pathways that may allow hydrocarbons and fracking chemicals to contaminate groundwater aquifers (Myers, 2012; Rodriguez et al., 2020; Vengosh et al., 2014); however, sealing may reduce fracture propagation and the possible migration of undesired fluids. Moreover, the low permeability of shale makes it a great candidate to act as cap-rock layers for carbon dioxide (CO_2) sequestration thus necessitating fracture remediation to ensure formation impermeability (Phillips, Lauchnor, et al., 2013). Additionally, fracking and horizontal drilling recover only a small percentage of the available hydrocarbons in a reservoir. But, if fractures can be sealed, wells may be restimulated

to enhance hydrocarbon recovery, in turn extending the life and efficiency of existing and future wells (i.e., “frack/re-frack”).

Existing Technologies to Seal Leakage Pathways

A host of technologies exist to seal unwanted leakage pathways in the subsurface that replace conventional squeeze cementation methods (Jafariesfad et al., 2020). This includes fine cement, commercially available resins (Todorovic et al., 2015), designer nanomaterials (Genedy et al., 2017; Genedy et al., 2019), and geopolymers (Hajiabadi et al., 2023). Most of these technologies, especially traditional Portland cement, are characterized by high viscosity fluids that cannot penetrate micro-scale fractures making it difficult to seal minute leakage pathways.

This research assesses the efficacy of sealing fractured shale with the bio-mineralization (or bio-cementation) technology known as Ureolysis-induced calcium carbonate precipitation (UICP). Characterized by low viscosity fluids and microscopic cementation agents (~2 μm), UICP can penetrate and seal leakage pathways on the order of 100 μm or smaller (Cunningham et al., 2019; Phillips, Gerlach, et al., 2013; Skorupa et al., 2019). Not only is UICP an advantageous cementing option for a variety of fracture sizes, but it also mimics natural fracture sealing found in subsurface shale. Calcite is the most common fracture-filling mineral to naturally form in subsurface shale fractures and is proven durable over a geologic timescale (Gale et al., 2014; Scotchman, 2016).

Background

UICP

Overview. Ureolysis-induced calcium carbonate precipitation (UICP) is a cementing technology that harnesses bio-chemical processes and results in the formation of calcium carbonate ($CaCO_3$). A source of urease enzyme is required to facilitate UICP-based technology which is found prevalently in nature in a variety of bacteria, algae, plants, and fungi (Krajewska, 2009). Microbially induced calcium carbonate precipitation (MICP), a subset of UICP, occurs when microorganisms (i.e., bacteria and/or algae) facilitate calcite precipitation. MICP results when metabolic activity, such as photosynthesis, sulfate reduction, nitrate reduction, or urea hydrolysis (ureolysis), causes an increase in the saturation state of $CaCO_3$ (Phillips, Gerlach, et al., 2013). The work presented here facilitates ureolysis using *Sporosarcina pasteurii*, a non-pathogenic, ureolytic soil bacteria commonly used in UICP applications due to its high urease concentrations (Mobley & Hausinger, 1989; Phillips, Gerlach, et al., 2013).

Chemistry and Applications. UICP occurs through a series of biochemical reactions that are outlined in Equations 1.1 – 1.6. The reactions begin when the urease enzyme facilitates ureolysis by converting urea and water into ammonia and carbamic acid (Equation 1.1). Spontaneously, further hydrolyses reactions convert carbamic acid to carbonic acid (Equation 1.2) and ammonia to ammonium and hydroxide (Equation 1.3). This increases the pH of the system, causing the dissociation of carbonic acid and the formation of bicarbonate (Equation 1.4) and carbonate (Equation 1.5). Finally, if sufficient calcium is present, calcium carbonate biomineral precipitation may form (Equation 1.6) (Phillips, Gerlach, et al., 2013).

$$CO(NH_2)_2 + H_2O \rightarrow NH_2COOH + NH_3 \qquad \text{(Equation 1.1)}$$

$NH_2COOH + H_2O \rightarrow NH_3 + H_2CO_3$ (Equation 1.2)

$2NH_3 + 2H_2O \leftrightarrow 2NH^{4+} + 2OH^-$ (Equation 1.3)

$H_2CO_3 \leftrightarrow HCO^{3-} + H^+$ (Equation 1.4)

$HCO^{3-} + H^+ + 2OH^- \leftrightarrow CO_3^{2-} + 2H_2O$ (Equation 1.5)

$Ca^{2+} + CO_3^{2-} \leftrightarrow CaCO_3$ (s) (Equation 1.6)

Phillips et al. (2013) reviews an array of engineering potentials for UICP application. Applications pertinent to this thesis include remediation related to hydraulic fracturing, enhanced oil and gas recovery, and improving caprock integrity for geologic carbon dioxide sequestration (Achal et al., 2015; Cunningham et al., 2019; Krajewska, 2018; Phillips, Lauchnor, et al., 2013; J. Y. Wang et al., 2014). Importantly, UICP is capable of remediating undesired leakage pathways in the field within wellbore cement fractures (Kirkland et al., 2021; Kirkland et al., 2020; Phillips et al., 2016; Phillips et al., 2018) and sandstone fractures (Cuthbert et al., 2013). Moreover, there is abundant evidence that UICP increases compressive strength in unconsolidated, porous media like sand and soil (Cui et al., 2017; Halder et al., 2014; Montoya & DeJong, 2015; Park et al., 2014; Xiao et al., 2019; Yasuhara et al., 2012) and has been used to increase the strength of concrete building materials (Bu et al., 2018; Cheng et al., 2020). UICP's past successes in fracture sealing, permeability reduction, and geomechanical property modification show promise that similar successes will be found in fractured shale.

Effect of Elevated Temperature on UICP. Temperature is a critical variable that influences UICP technology (Wang et al., 2023); moreover the variable depth and elevated temperature range of subsurface shale presents a host of challenges that may affect the viability of UICP. Temperature influences microbial growth/death, urease activity/inactivation, and kinetic

ureolysis rates, as well as calcite precipitation rates, quantity, and morphology. Biomineralization is well researched and applied at temperatures ranging from 20 - 30°C; however, administering UICP to engineering applications at elevated temperatures is less established. The work presented here investigates UICP's ability to seal leakage pathways at 60°C in fractured shale. Sixty degrees Celsius was chosen because it mimics the temperature of shallow subsurface shale plays and promotes rapid ureolysis rates. *S. pasteurii* microbes become unculturable at 60°C but their urease enzyme remains active, allowing biomineralization to transpire (Skorupa et al., 2019). A variety of sources validate urease activity at temperatures ranging from 10 - 80°C, showing activity peaking around 60°C (Akyel, 2022; Feder et al., 2021; Illeová et al., 2003; Illeova et al., 2020; Ng et al., 2012; Sahrawat, 1984).

Previous studies have shown that elevated temperatures cause increasingly fast ureolysis rates and potential enzyme inactivation (Akyel, 2022; Feder et al., 2021; Illeová et al., 2003; Illeova et al., 2020). Feder et al. (2021) used jack bean meal (JBM), a plant-based source of urease, to study temperature-dependent ureolysis rates and urease enzyme inactivation. Ureolysis was investigated at temperatures between 20 - 80°C showing that rates increased as temperatures increased. The optimum temperature for ureolysis rates occurred around 60°C where the urea in the system (20 g/L) was completely hydrolyzed within 60 minutes. However, when temperatures exceeded 60°C, ureolysis ceased within 20 – 30 minutes with excess unhydrolyzed urea remaining in the system. Separately, to determine enzyme inactivation, JBM was exposed to temperatures ranging 50 - 80°C where inactivation rates and temperatures simultaneously increased resulting in a decrease in urease half-life ($t_{1/2}$) (Table 1.1). Here, half-life references the amount of time needed for the concentration of urease to decline by 50%.

In another study, Akyel (2022) compared the enzyme thermal inactivation and reaction rates of urease sourced from *S. pasteurii* to the JBM urease activity results determined by Feder et al. (2021). Table 1.1 presents the half-lives of each urease source for temperatures ranging from 50 - 80°C. Like JBM-urease, ureolysis reaction rates using *S. pasteurii*-urease increased as temperature increased. Furthermore, urease was found to inactivate rather quickly and unable to utilize all available urea (20 g/L) at temperatures beyond 70°C. This illustrates a similar temperature-dependency for both urease sources.

Table 1.1. Temperature dependent half-lives ($t_{1/2}$) for Jack Bean Meal (JBM)-urease (from Feder et al., 2021)) and *S. pasteurii*-urease (from Akyel, 2022)) for temperatures between 50°C - 80°C.

	Jack Bean Meal-urease Feder et al. (2021)	*S. pasteurii*-urease Akyel (2022)
Temperature [°C]	$t_{1/2}$ (min)	$t_{1/2}$ (min)
50	2238	2182
55	835	-
60	317	461
65	125	-
70	62	66
75	26	-
80	5	5

Although ureolysis rates peak around 60°C, there is evidence that mineral precipitation is optimized at lower temperatures. Kim et al. (2018) observed temperature's effect on MICP comparing two species of ureolytic bacteria, *Staphyloccoccus saprophyticus* and *Sporosarcina pasteurii*, at 20, 30, 40, and 50°C. For both species they concluded that maximum precipitation occurs at 30°C, while the precipitation at higher temperatures significantly declines by 60-70%.

Cheng et al. (2017) investigated the unconfined compressive strength of silica sand columns stabilized with MICP under various temperature conditions (4°C, 25°C, and 50°C) and found that calcite formed at 50°C achieved the lowest strength improvement due to ineffective calcite precipitation. They studied the kinetics of crystallization, specifically the relationship between competing kinetic rates of nucleation and crystal growth. Scanning electron microscopy SEM) technology was used to characterize the shape and location of $CaCO_3$ precipitation. They found excess nucleation sites when MICP was performed at 50°C and an average crystal size of 2-5 μm. This was found to be 10x smaller than the average crystal size of MICP performed at 25°C (20 - 50 μm). Microstructure analysis of experiments run at 50°C showed crystals spatially well-distributed, applying a coating-like layer on sand grains; however, large gaps were observed between grains, meaning they were not effectively connected with precipitation. This paper suggested performing MICP at 25°C to improve the compressive strength of treated sand columns because at 25°C larger calcite crystals will form with fewer nucleation sites allowing precipitation to fill gaps between sand grains.

Wang et al. (2023) explored how temperatures ranging from 4 - 50°C influence MICP characteristics such as bacterial activity, growth and attachment, as well as crystal (precipitation) growth, dissolution, shape, size, and transform efficiency by performing bacterial activity batch

tests and microfluidic chip experiments. Microfluidic chips were designed to represent a two-dimensional model of realistic, porous soil medium based on a cross-sectional image of Ottawa 50 - 70 sand. Bacterial attachment on the microfluidic chips was monitored using images taken by an optical microscope after completing the MICP treatment procedures. They found optimal bacterial growth and bacterial attachment occur at 20°C and 35°C, respectively. However, although they observed the initial precipitation rate increasing exponentially as temperature increased, the precipitation efficiency of MICP was lower at 50°C because, consequently, microbial density and activity was reduced.

In a field demonstration, Kirkland et al. (2021) successfully utilized UICP in the presence of CO_2-affected brine to seal an undesired fracture in a cement wellbore annulus. More applicably to this thesis, *S. pasteurii* cultures were heat-treated to 60°C prior to subsurface injection, with the intention of mimicking deeper subsurface temperature conditions where microbe survival is questionable. At 60°C, *S. pasteurii* cells become inactivated while maintaining their urease enzyme activity. Although ureolysis rates were higher in heat-treated, inactivated cultures, the resulting biomineral seal was found to be less robust compared to another fracture in the same well sealed using live microbes at ambient temperatures and without the presence of CO_2-affected brine. It is undetermined if the presence of CO_2-affected brine or heat-treated, inactivated microbes is the cause of the weaker seal.

As previous research shows, temperature is an influential parameter on the behavior of biomineralization. Clearly it is possible to create calcite precipitation and seal leakage pathways in cement when microbial cultures (*S. pasteurii*) are exposed to temperatures at or approaching

60°C. However, the question remains, will UICP be effective and prove strong enough to seal fractured shale at 60°C?

UICP in Fractured Shale. As mentioned, naturally forming calcite precipitation is a common cementing agent that develops within naturally occurring subsurface shale fractures. Utilizing engineered calcite precipitation to treat and seal hydraulically induced fractured shale is an emerging application of UICP. However, limited studies have attempted to treat fractured shale with biomineral. The variable depth and increased temperature range of subsurface shale formations presents a host of challenges affecting the viability of UICP. Sealed leakage pathways may be achieved after multiple injections of microbial cultures and mineral-promoting fluids precipitate enough calcite to bridge the fracture, fill the void, and reduce the permeability in the fracture.

Cunningham et al. (2015) biomineralized three Opalinus shale cores sourced from Switzerland's Mont Terri test site. All UICP treatments were administered under ambient temperature conditions. Two of the cores were biomineralized under ambient pressure conditions, achieving a permeability decrease in the fracture up to four orders of magnitude. The remaining core was biomineralized at a high overburden pressure that mimics what is possible in the subsurface at Mont Terri (61.2 bar or 6.12 MPa or 900 psi), and the result was one order of magnitude permeability reduction.

Another study successfully applied UICP treatments at 60°C and 70°C to fractured shale until permeability in the fracture was reduced by three to four orders of magnitude (Hiebert, 2019). Furthermore, the sealed shale was pulled apart and new fractures were created in the shale

rock rather than the original fracture sealed with biomineral. Though not further explored, this finding indicates UICP's potential to alter the mechanical properties of fractured shale.

Most recently, Willett et al. (2023) obtained three orders of magnitude permeability reduction after delivering UICP treatment to a fractured shale core at 60°C. The core was cylindrical (5.08 cm long by 2.54 cm diameter) with a single fracture spanning the entire length of the core. Notably this study uses non-invasive tools, specifically nuclear magnetic resonance (NMR) and micro-X-ray computed tomography (μ-CT), to assess the extent of biomineralization within the fracture. Results indicated calcite deposits bridging the gap between shale pieces creating an intact, free-standing composite core.

Results of these studies indicate UICP's potential to seal fractures in shallow subsurface shale formations. What is still needed is an understanding of how the mechanical properties change between intact (unfractured) shale and fractured shale sealed with biomineralization. If biomineralization can bridge the gap in fractured shale and prove strong enough to seal fractures at the laboratory scale, UICP treatments may be used at the field scale to remediate undesired leakage pathways, limit fracture propagation, better store carbon dioxide, and extend the life and efficiency of existing and future wells.

Mechanical Testing

Tensile Testing Methods.

Tensile strength is a fundamental mechanical property used to characterize rock failure. There is evidence that tension is a common failure mode for subsurface fracture opening and propagation induced by hydraulic fracturing (Ferrill et al., 2014; Holt et al., 2015). Moreover, it is meaningful for hydraulic fracturing design and predicting fracture patterns

(Li et al., 2021). Tensile testing assesses the strength and ductility of a material when a specimen is pulled or stretched until it breaks or fractures (Dowling et al., 2019).

Direct tensile strength (DTS) testing offers the most accurate and reliable interpretation of tensile strength; however, it is notoriously difficult and expensive to administer routinely (ASTM, 2016). In accordance with ASTM D2936-20, the Standard Test Method for Direct Tensile Strength of Intact Rock Core Specimens, flat faces of a rock core (cylindrical) or block are adhesively attached to metal caps in which the specimen can be held in the test apparatus, and a direct tensile load is applied until the specimen fails (ASTM, 2008). Simply put, a specimen is gripped at two ends and pulled apart. However, due to difficult sample preparation and experimental procedures, DTS tests are seldom administered. In lieu of direct methodology, rock tensile strength can be determined using a variety of indirect methods, such as the ring test (Chen & Hsu, 2001), the Luong core test (Wang et al., 2020), the pull-off test (Cacciari & Futai, 2018; Vizini et al., 2020), the bending test (Liao et al., 2019), and the Brazilian test (Efimov, 2021). The Brazilian indirect tensile strength test was chosen for this research due to its simplicity and efficiency.

Brazilian Indirect Tensile Strength (BITS) Methodology. The BITS methodology is a widely used alternative for assessing the tensile strength of rock. Standard method nomenclature designates BITS results as the “splitting tensile strength” of rock (ASTM, 2016). Unlike DTS testing, BITS requires simple test administration and straightforward sample preparation, where no adhesive procedures are required. Tensile failure is promoted when an unconfined compressive load is applied to a cylindrical disc-shaped rock specimen until it splits apart (Figure 1.4). BITS tests induce tensile stresses perpendicular to the loading diameter causing the

specimen to break, or "split apart," diametrically (ASTM, 2016; Li & Wong, 2013). BITS is desirable for this research because it is a simple test that can mimic complicated stress fields where combinations of compressive and tensile stress fields coexist.

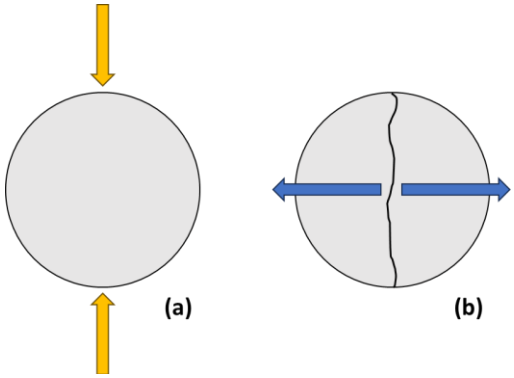

Figure 1.4. Brazilian indirect tensile test schematic. (a) An unconfined compressive load (yellow vertical arrows) is applied to a disc-shaped specimen, inducing tensile stresses. (b) The specimen splits apart perpendicular (blue horizontal arrows) to the applied compressive load.

Splitting tensile strength is calculated using Equations 1.7 and 1.8, accounting for the use of either flat platens or curved platens, respectively. Platens are the pieces of the testing apparatus that contact the specimen. Curved platens were chosen for this research as this geometry reduces the stress concentration at loading points on the specimen (ASTM, 2016; Mellor & Hawkes, 1971).

$$\sigma_t = 2P / \pi tD \quad \text{(Equation 1.7)}$$

$$\sigma_t = 1.272P / \pi tD \quad \text{(Equation 1.8)}$$

Where σ_t is the splitting tensile strength (MPa or psi), P is the maximum applied load indicated by the testing machine (N or lbf), t is the thickness of the specimen (mm or in), and D is the diameter of the specimen (mm or in).

Brazilian Indirect Method in Shale. Numerous studies have evaluated the splitting tensile strength of intact shale discs using BITS. Shale tested under Brazilian conditions was found to have 4 different failure modes (Bisai & Chakraborty, 2019). Figure 1.5 provides a visual guide to the failure modes as follows: (a) the central (vertical) fracture consisting of a single fracture in the middle of the specimen, (b) a singular non-central fracture in which the fracture does not intersect the core diametrically through the middle of the specimen, (c) layer activation where fractures occur in-line (horizontal), or parallel, with the splitting plane, and (d) multiple central fractures occurring vertically in the central region of the specimen.

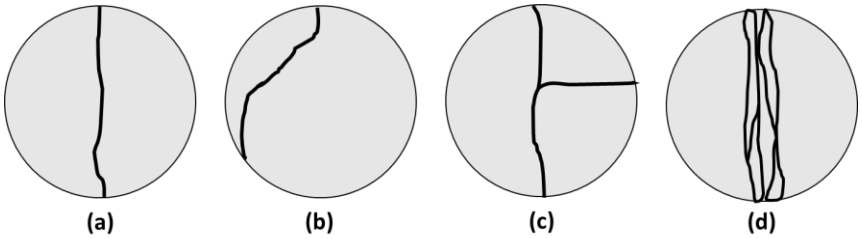

Figure 1.5. Failure modes associated with BITS testing. (a) central fracture (b) non-central fracture (c) layer activation (d) multiple central fractures. Modified from Bisai & Chakraborty (2019).

Li et al (2017) performed BITS tests on Eagle Ford and Mancos shale samples to investigate the effects of pre-existing fractures, mineralogy, bedding-plane orientation and laminations, and water content. X-ray powder diffraction (XRD) analysis found the Eagle Ford shale used in this study to be carbonate dominated (approximately 62.2% calcite) with an average mineral content similar to what is represented on Figure 1.3. The Mancos shale (not represented in Figure 1.3) was found to be silicate dominated (approximately 48.4% quartz) with a clay content four times higher than that of Eagle Ford. They determined that pre-existing microfractures, detected via X-ray CT scanning, can reduce tensile strength up to 66%.

Additionally, tensile strength decreased as water content increased. The splitting tensile strength of Eagle Ford was significantly impacted by bedding plane/laminations, but the same was not found for Mancos. Eagle Ford was found to be more brittle with a low clay content (approximately 6%) and tended to break with the multiple central fractures or layer activation failure modes. Comparatively, the Mancos clay content was much higher (approximately 22%) primarily resulting in singular central fracture breakage of the specimens. Their results indicated that a higher clay content decreases the overall tensile strength and might be the reason for different fracture patterns found between the two shale types.

Many researchers have investigated shale's anisotropic behavior during BITS testing by studying the effects of bedding plane, orientation of laminations, and/or loading orientation (Gao et al., 2015; He & Afolagboye, 2018; Hou et al., 2018; Mokhtari et al., 2014; Simpson et al., 2014; Wang et al., 2016). The effects of thermally conditioned linear fracturing fluid and reservoir temperature-controlled conditions were investigated on the tensile strength of both Eagle Ford and Wolfcamp shales (Iferobia et al., 2022). Results from these studies suggest temperature, orientation, bedding plane, water content, mineralogy, and pre-existing microfractures can greatly influence the resulting mechanical properties of shale.

Scope

Gaps

UICP technology is currently deployed in the subsurface to seal unwanted fractures in sandstone and cement wellbore casings; however, UICP's efficacy to seal fractured shale remains unknown. This research investigates UICP's ability to seal fractured shale cores and evaluates tensile strength of the resulting composite cores. Additionally, it compares tensile strength of

intact shale cores versus fractured cores sealed with UICP. The work presented here is the first step towards understanding how UICP modifies the mechanical properties of fractured shale for future field-scale applications.

Thesis Outline

Chapter two contains the published, peer-reviewed conference paper, "Developing Methods to Assess Changes in Mechanical Properties of Shale Modified by Engineered Mineral Precipitation," prepared for the 57th U.S. Rock Mechanics Geomechanics Symposium hosted by the American Rock Mechanic Association held in Atlanta, Georgia, USA in June 2023. It outlines developed tensile strength testing methods on intact (unfractured) shale cores with the intention of using those methods to inform the results of shale cores fractured and sealed with UICP. Tensile tests were performed on two types of shale comprised of different mineral content, Eagle Ford and Wolfcamp (Figure 1.3). Both shale types were tested at room temperature and 60°C. This work compares how shale type and temperature influence tensile strength.

Chapter three contains the manuscript, "Splitting Tensile Strength of Fractured Shale Cores Sealed with UICP," and is ready for future submission. Two different biomineralization delivery methods to seal fractured shale cores are presented: 1) the flow-through method that injects UICP promoting solutions into a fractured shale core in a sequential pattern of microbes followed by urea and calcium-containing media and 2) the immersion method that places fractured cores treated with guar gum and UICP promoting solution in a batch reactor, which is allowed to incubate over time. Results include a comparison of biomineralization methods in terms of the tensile strength of sealed cores. The methods developed in chapter two were used to

assess tensile strength in the specimens discussed in chapter three. Chapter three is the first step towards determining if guar gum would be a suitable additive to UICP technology.

Chapter four summarizes conclusions from chapters two and three. It compares the tensile strength of intact shale cores versus shale cores fractured and sealed with UICP and provides concluding remarks addressing the significance of all results in this thesis in terms of UICP treatment efficacy. Additionally, recommendations for future research wrap up chapter four and the thesis in entirety.

CHAPTER TWO

DEVELOPING METHODS TO ASSESS CHANGES IN MECHANICAL PROPERTIES OF SHALE MODIFIED BY ENGINEERED MINERAL PRECIPITATION

Contribution of Authors and Co-Authors

Manuscript in Chapter 2

Author: Kayla Bedey

Contributions: Experimental design, data collection, data analysis, writing.

Co-Author: Matthew R. Willett

Contributions: Editing.

Co-Author: Laura Dobeck

Contributions: Experimental design.

Co-Author: Joe Eldring

Contributions: Experimental design, editing.

Co-Author: Dustin Crandall

Contributions: Project sponsor, editing.

Co-Author: Jonny Rutqvist

Contributions: Project sponsor, editing.

Co-Author: Al Cunningham

Contributions: Experimental design, editing.

Co-Author: Catherine M. Kirkland

Contributions: Experimental design, writing, editing.

Co-Author: Adrienne J. Phillips

Contributions: Experimental design, writing, editing.

Manuscript Information

Kayla Bedey, Matthew R. Willett, Laura Dobeck, Joe Eldring, Dustin Crandall, Jonny Rutqvist,

Al Cunningham, Catherine M. Kirkland, Adrienne J. Phillips

American Rock Mechanics Association Conference Proceedings

Status of Manuscript:
☐ Prepared for submission to a peer-reviewed journal
☐ Officially submitted to a peer-reviewed journal
☐ Accepted by a peer-reviewed journal
☒ Published in a peer-reviewed journal

OnePetro
Paper presented at the 57th U.S. Rock Mechanics/Geomechanics Symposium, Atlanta, Georgia, USA, June 2023
DOI: 10.56952/arma-2023-0807

Abstract

Fractures in subsurface shale formations serve multiple purposes, for example, in the recovery of resources in hydraulic fracturing or as potential harmful leakage passages through caprocks that may contribute undesired fluids to the atmosphere or functional groundwater aquifers. A proposed method to seal or influence fracture properties is Ureolysis-Induced Calcium Carbonate Precipitation (UICP), a bio-mineralization technology driven by the enzymatic hydrolysis of urea, resulting in the formation of calcium carbonate. The resulting calcium carbonate can bridge the gaps in fractured shale and reduce fluid flow through fractures. This study represents the first step toward determining the influence of UICP treatment on shale material and its subsequent mechanical strength properties. The goal of this preliminary work is twofold: first, we aim to identify a method to test tensile strength along a core axis and second, we seek to assess the effect of temperature on the tensile strength of intact, unfractured shale cores (2.54 cm (1 in) diameter, 5.08 cm (2 in) long for comparison with future fractured and UICP-treated cores. A modified Brazilian indirect tensile strength test successfully measured splitting tensile strength of shale cores from Eagle Ford and Wolfcamp formations at room temperature and 60°C.

Introduction

Hydraulic fracturing coupled with horizontal drilling has been an instrumental technology for extraction of natural gas reserves in subsurface rock formations such as sandstone and shale. Shale gas is the natural gas trapped within subsurface shale formations and has become a crucial unconventional energy source amid an evolving energy landscape. Hydraulic fracturing and horizontal drilling stimulated energy independence, lowered fuel prices, and promoted job

creation in the United States (Q. Wang et al., 2014). While hydraulic fracturing created many positive economic impacts, it has also generated undesirable environmental effects. This research is aims at offsetting environmental costs by sealing fractured subsurface shale using a sustainable bio-mineralization technology known as Ureolysis-induced calcium carbonate precipitation (UICP) (Kirkland et al., 2021). If UICP can bridge the gap in fractured shale, and prove strong enough to seal fractures, UICP treatments may be used at the field scale to limit fracture propagation, better store carbon dioxide, and extend the life and efficiency of existing and future wells.

Moreover, better understanding how UIPC alters the material and mechanical properties of fractured shale will allow improved exploitation of domestic energy resources like shale gas. In concurrent research, UICP has proven to reduce permeability through shale fractures (M. R. Willett et al., 2023). What is now needed is an understanding of how UCIP alters the mechanical properties of fractured shale cores. Comparison of tensile strength before and after sealing will determine how mechanical properties change as the result of UICP treatment. This project is in partnership with the Lawrence Berkeley National Laboratory where the resulting mechanical properties of UICP treated shale will inform the geo-mechanical modeling efforts.

Tensile Strength Testing

Tensile strength is a fundamental mechanical property used to characterize rock failure. Direct tensile strength (DTS) testing offers the most accurate and reliable interpretation of tensile strength, using fewer assumptions and offering direct physical meaning of the deformation and failure characteristics of rocks in tension (Hashiba et al., 2017). To determine direct tensile strength, a specimen is gripped at two ends and pulled apart. However, it is uncommon to

administer these tests due to difficult sample preparation and experimental procedures. Indirect methods are more commonly utilized to evaluate the tensile strength of rock. A plethora of indirect methods are available to determine the tensile strength of rock, such as the ring test (Chen & Hsu, 2001), the pull-off test (Cacciari & Futai, 2018), the Luong core test (Wang et al., 2020), the bending test (Liao et al., 2019), and the Brazilian test (Efimov, 2021). Along with a modified direct tension test, the Brazilian indirect tensile strength (BITS) test was used in this study.

The Brazilian indirect tensile strength test is a widely used method for determining the splitting tensile strength of rocks. BITS is a popular testing option because it offers easy sample preparation and simple test administration. The splitting tensile strength is obtained by applying a compressive load onto a specimen (Figure 2.1b and c). This load induces tensile stresses normal to the vertical diameter and the specimen "splits" apart (Li & Wong, 2013). To calculate the indirect tensile strength, failure is assumed to occur at the point of maximum tensile stress, which is assumed to be at the center of the specimen (Li & Wong, 2013).

BITS with Shale

Numerous studies have evaluated the splitting tensile strength of shale using BITS. Shale under indirect tension was found to have different failure modes and fracture patterns (Bisai & Chakraborty, 2019). Li et al. (2017) performed BITS tests on Eagle Ford and Mancos shale samples to investigate the effects of pre-existing fractures, mineralogy, bedding-plane orientation and laminations, and water content. Many researchers have investigated shale's anisotropic behavior during BITS testing by studying the effects of bedding plane, orientation of laminations, and/or loading orientation, (Gao et al., 2015; He & Afolagboye, 2018; Hou et al.,

2018; Mokhtari et al., 2014; Simpson et al., 2014; Wang et al., 2016). The effects of thermally conditioned linear fracturing fluid and reservoir temperature-controlled conditions were investigated on the tensile strength of both Eagle Ford and Wolfcamp shales (Iferobia et al., 2022). Results from these studies suggest temperature, orientation, bedding plane, water content, mineralogy, and pre-existing microfractures can greatly influence the resulting mechanical properties because of shales' anisotropic nature.

UICP Core Treatment

Ureolysis-induced calcium carbonate precipitation (UICP) is a cementing agent that harnesses bio-chemical processes and results in the formation of calcium carbonate ($CaCO_3$). Over a short reaction period (hours), calcium carbonate will precipitate in fractures or the pore spaces of rocks. Phillips et al. (2013) reviews the wide span engineering potentials of UICP application. Most relevant to the future of this study relate to energy sector applications like wellbore cement sealing (Phillips et al., 2018) and improving caprock integrity for geologic carbon dioxide sequestration (Phillips, Lauchnor, et al., 2013; J. Y. Wang et al., 2014). Previous research at Montana State University has demonstrated that UICP can seal fractures in sandstone (Phillips et al., 2016) and shale (Cunningham et al., 2015; M. R. Willett et al., 2023). There is also abundant evidence the UICP increases compressive strength in unconsolidated media like sands and soil (Cui et al., 2017; Halder et al., 2014; Montoya & DeJong, 2015; Park et al., 2014; Xiao et al., 2019; Yasuhara et al., 2012) and can be used to increase the strength of building materials like concrete (Bu et al., 2018; Cheng et al., 2020).

Fracture sealing, permeability modification, and the geo-mechanical properties of rocks can be influenced by the injection of mineralization-promoting fluids into the rock or its fractures

(Cunningham et al., 2014). With all the available evidence suggesting that UICP can seal fractures in rock and alter mechanical properties in porous media, what is needed now is an examination of how UICP treatment influences the material (M. R. Willett et al., 2023) and mechanical properties, particularly, the tensile strength of shale rocks relevant for the energy sector. This methods development study is aimed at better understanding the mechanical properties of shale rock when it is optimized for UICP treatment to allow for improved exploitation of domestic energy resources like oil and natural gas.

Motivation

The first objective of the study was to experimentally assess the methods to fracture intact shale cores (5.08 cm long, 2.54 cm diameter) using the BITS and DTS test methods. The second objective was to assess the effect of temperature on the splitting tensile strength between intact cores tested at ambient room temperature and 60°C for two different shale types. Though 60°C may not mimic actual subsurface temperatures of the shales used in this study, it was chosen because it approaches subsurface temperatures for shallow shale plays and promotes rapid ureolysis rates during UICP treatment of the fractured cores to be tested later in the study. Results from this study will indicate how to test the tensile strength of fractured shale cores modified with UICP treatment, both with respect to the testing method and testing temperature. It is important to evaluate the fracture capability of intact shale as a benchmark for comparison with how shale behaves after it is fractured and sealed with UICP to better inform modeling efforts.

Methods and Materials

Core Sample Preparation

A total of 21 cores were used in this study, originating from two large, commercially drilled shale rock formations in Texas (Kocurek Industries, Inc.). One Eagle Ford core was used for the DTS test. Ten Eagle Ford cores and 10 Wolfcamp cores were used for BITS testing. All samples were cored parallel to the bedding plane. This research uses a different geometry than typically seen in BITS testing and is modified from the ASTM standard. UICP shale samples were cored to approximately 5.08 cm (2 in) long by 2.54 cm (1 in) diameter resulting in a length to diameter ratio of 2.0, Figure 2.1a shows a Wolfcamp core demonstrating the geometry used in this study. For this study, sample geometry was optimized for future UICP treatment and experimentation, calling for a modification in BITS testing standards. Typically, disc-shaped samples with a ratio of 0.2 - 0.75 are used for compliance with ASTM (ASTM, 2016). All cores were weighed, oven dried for a minimum of 24 hours, and weighed again before testing to ensure a constant weight and lack of moisture in pore spaces.

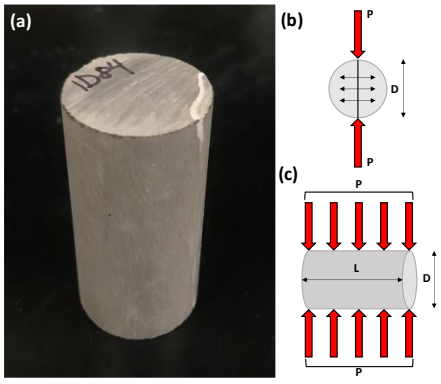

Figure 2.1. (a) Wolfcamp shale core demonstrating the geometry used in this study, 5.08 cm length, 2.54 cm diameter. (b) Plan view of BITS where P is the applied compressive load. (c) Side view of BITS test on sample with a 2.0 length to diameter ratio.

Core Testing

BITS testing was performed using an MTS Criterion Model 43 Electromechanical Test System with an environmental chamber (Figure 2.2) using a load cell with a maximum rated force capacity of 30 kilonewton (kN) [6600 lbf]. Core specimens were loaded to failure and load versus deformation curves and maximum applied load values were recorded.

Ten cores (five Eagle Ford and five Wolfcamp) were used for room temperature or 60°C tests. For the 60°C tests, the environmental chamber surrounding the MTS testing system (Figure 2.2b) was pre-heated to temperature (60°C) and the cores were placed inside the chamber for a 3-hour equilibration period to ensure homogeneous heat distribution throughout the samples.

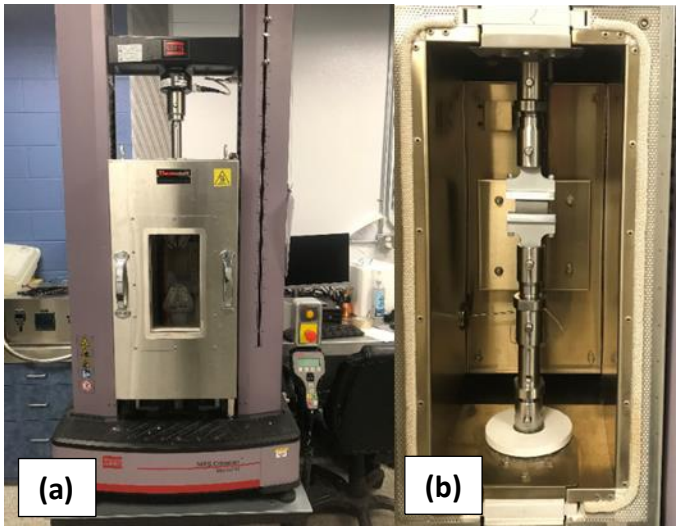

Figure 2.2. BITS testing apparatus. (a) MTS Criterion Model 43 with environmental chamber. (b) Looking inside the environmental chamber at test fixture attached to MTS.

Two custom-made test fixtures (Figure 2.3) were fabricated at the Montana State University Machining Laboratory to accommodate the MTS testing apparatus. Figure 2.3a shows the fixture used to run a direct tension test. J-B Weld was used to attach the core to both sides of the test fixture and allowed to set for 24 hours before running the test. Figure 2.3b shows the

BITS test fixture used in this study. Adhesives were not necessary for BITS testing. Curved loading platens were chosen to reduce the stress concentration at the loading points (Mellor & Hawkes, 1971).

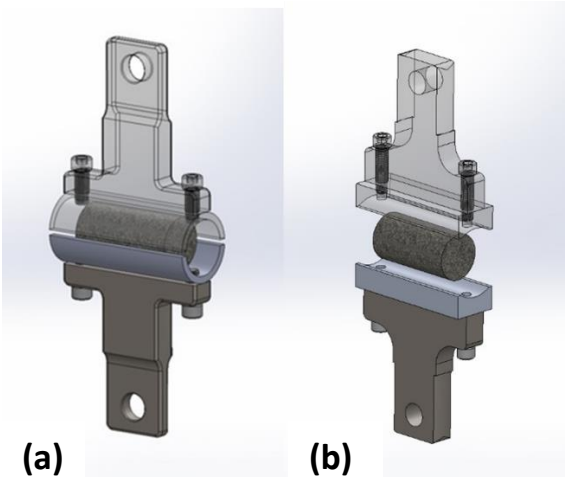

Figure 2.3. Test fixtures a) for DTS testing and b) for BITS testing.

Cores were loaded to failure at a rate of 100 N/s. The maximum load applied was used to calculate the splitting tensile strength of shale samples using Equation (2.1):

$$\sigma_t = 1.272P / \pi tD \qquad \text{(Equation 2.1)}$$

Where σ_t is the splitting tensile strength (MPa or psi), P is the maximum applied load indicated by testing machine (N or lbf), t is the thickness of the specimen (mm or in), and D is the diameter of the specimen (mm or in) (ASTM, 2016). Equation 2.1 is specific to BITS tests utilizing curved loading platens.

Results and Discussion

DTS Testing

Results of a DTS test were inconclusive due to the difficult nature of the test. Moreover, the unconventional core geometry proved problematic. A typical DTS test, following the ASTM standard (ASTM, 2008), would adhere the test fixture to the flat, circular faces of the specimen and pull it apart axially. However, because this study aims to develop methods to test future UICP-treated shale cores, it was necessary to orient the core horizontally lengthwise, so the tensile forces could be determined along the longitudinal axis. Figure 2.4 compares standard sample orientation for DTS testing (a) with orientation used in this study (b). Attaching the test fixtures to curved surface (instead of flat) calls into question the validity of a DTS and the resulting tensile strength. Upon completion of the test, it was suspected the epoxy to have reacted with the shale creating a failure at the bond-surface interface. The top of the core fixture broke away from the core (Figure 2.5) in 1.32 sec at a load of 0.271 kN. No further DTS tests were attempted. Due to the difficulty of administering a DTS test with the necessary core geometry and orientation, BITS testing was deemed a logical solution to determine the tensile strength of shale cores in this study.

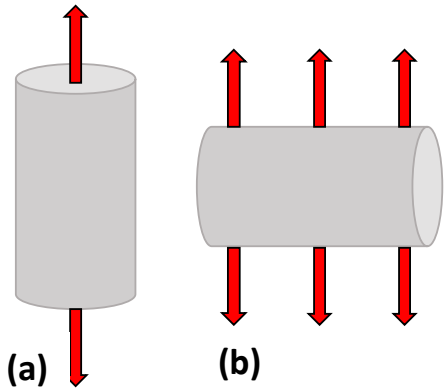

Figure 2.4. Orientation for direct tensile strength testing a) ASTM orientation and b) orientation used in the present study.

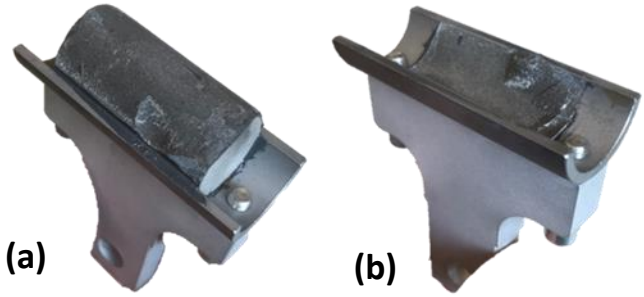

Figure 2.5. DTS results. There is assumed failure at the bond-surface interface. (a) Bottom test fixture. (b) Right is the top test fixture.

Splitting Tensile Strength and Fracture Pattern

Four sample groups (each with five replicates) were evaluated for splitting tensile strength using a modified BITS method. A value of five was chosen for replicates to account for statistical variation in shale. Group one contained samples of Eagle Ford shale (EF-45, EF-46, EF-53, EF-54, and EF-55) tested at room temperature resulting in an average tensile strength of 7.22 ± 0.55 MPa. Eagle Ford samples (EF-47, EF-49, EF-86, EF-88, and EF-89) in the second group were tested at 60°C resulting in an average tensile strength of 6.02 ± 0.55 MPa. The third group consisted of Wolfcamp cores (WC-62, WC-63, WC-65, WC-66, and WC-70) tested at room temperature where the average tensile strength was 6.07 ± 1.35 MPa. Group four tested

Wolfcamp samples (WC-67, WC-68, WC-69, WC-77, and WC-80) producing an average tensile strength of 5.46 ± 2.44 MPa. Figure 2.6 and Table 2.1 summarize and compare results of average tensile strength for each sample group.

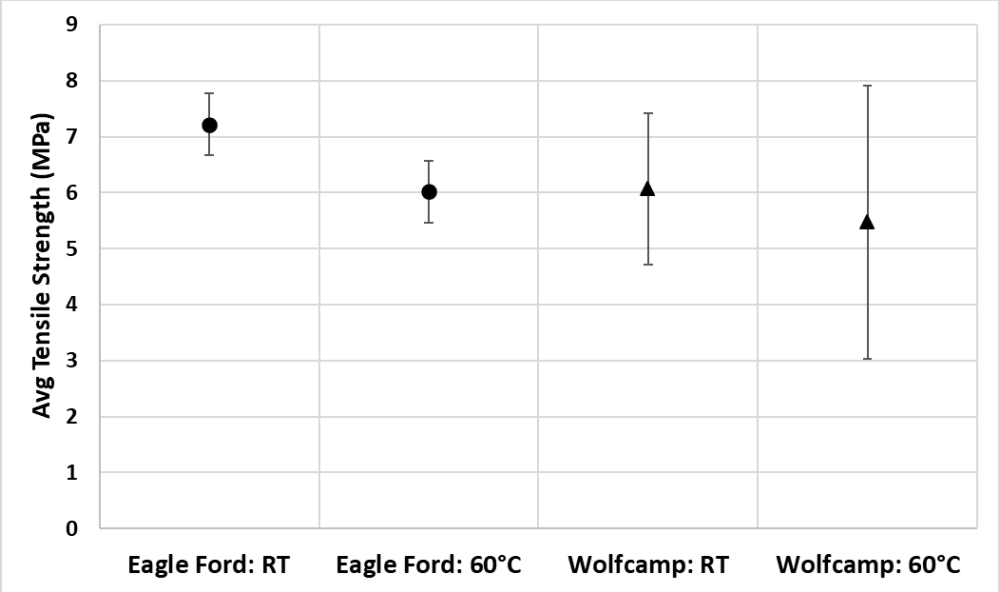

Figure 2.6. Average tensile strength (MPa) and standard deviation for each type of shale and temperature combination. Each group contains 5 replicates. Eagle Ford shale is represented by a circle and Wolfcamp shale is represented by a triangle.

Table 2.1. Average tensile strength (MPa) per sample group.

Shale Type: Temperature	Ave Tensile Strength (MPa)
Eagler Ford: Room Temp	7.22 ± 0.55
Eagle Ford: 60°C	6.02 ± 0.55
Wolfcamp: Room Temp	6.07 ± 1.35
Wolfcamp: 60°C	5.46 ± 2.44

All sample groups demonstrate variations in tensile strength between the 5 replicates. However, it was evident in this study that the tensile strength of Eagle Ford shale showed less variation between individual samples than Wolfcamp as can be seen in Figure 2.7. The average tensile strength of the five replicates for each of the Eagle Ford groups exhibited smaller standard deviation values than that of the Wolfcamp groups (Figure 2.6).

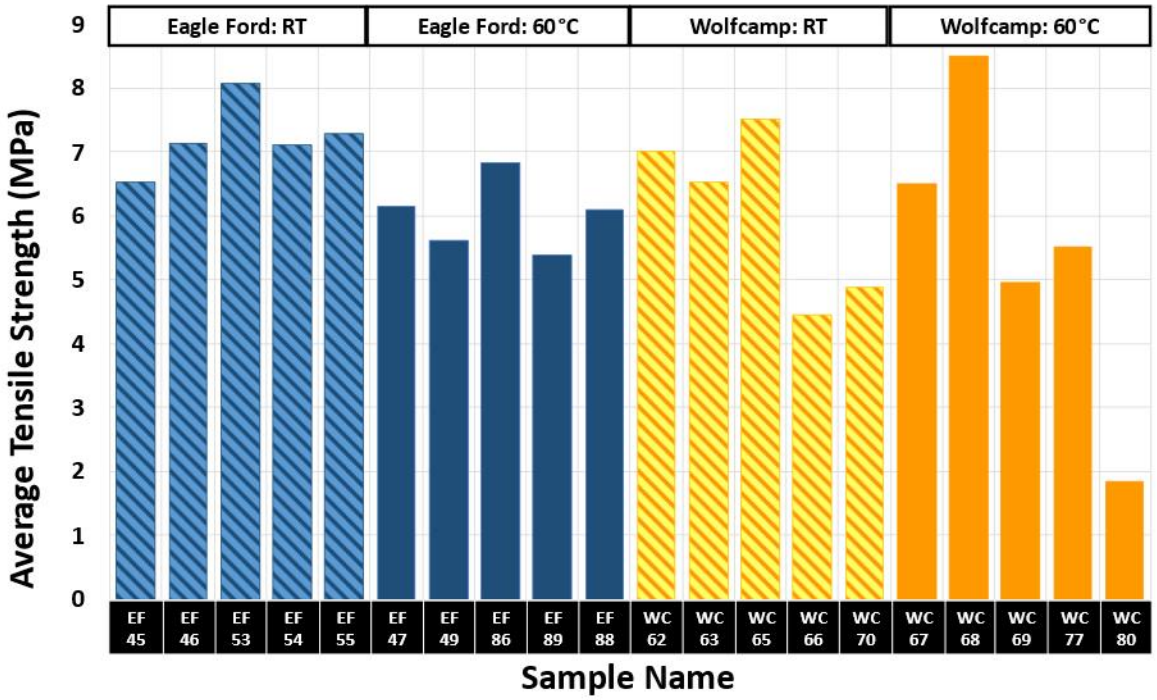

Figure 2.7. Comparison of tensile strength (MPa) of 20 intact shale samples tested using BITS. Blue bars with a sample name "EF" refer to Eagle Ford samples and yellow bars with a sample name "WC" represent Wolfcamp samples. Darker bars indicate samples tested at 60°C and lighter bars with dark diagonal lines indicate samples tested at room temperature.

As seen in Figure 2.7, Wolfcamp samples demonstrated more variability in tensile strength believed to be caused by the existence of visible fractures. Cores WC-66, 70, 77, and 80 contained visible fractures. Figure 2.8 exhibits cores WC-66 and WC-80 depicting representative visible fractures. The variability in tensile strength and existence of fractures could be the result

of sample coring procedures or the anisotropic nature of shale. No cores in this study were subject to preliminary CT scans so the existence of non-visible, internal micro-fractures is unknown. No Eagle Ford cores contained visible fractures. Li et al. (2017) found that the tensile strength of shale can be reduced up to 66% when pre-existing micro-fractures are detected and that bedding plane/laminations significantly impact Eagle Ford tensile strength. Wolfcamp shale was not tested in their study, but this study found cores with existing fractures greatly influenced the standard deviation of average tensile strength.

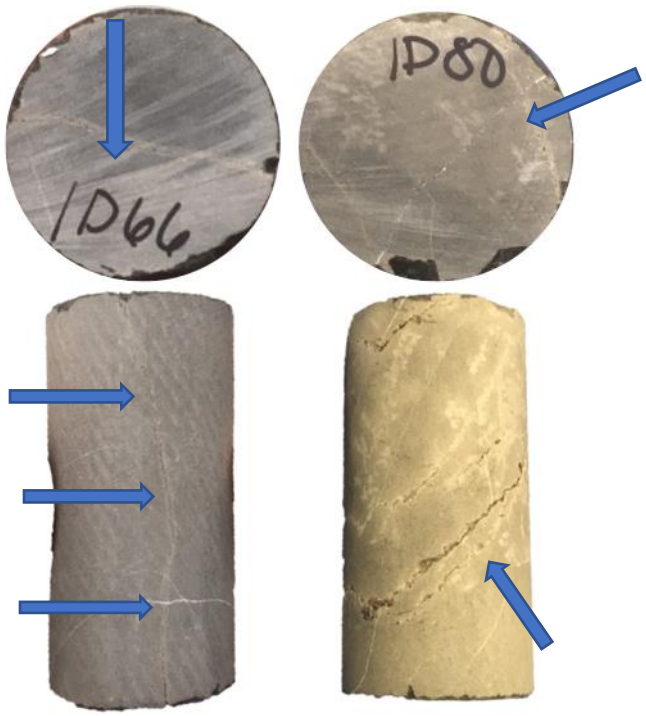

Figure 2.8. Representative Wolfcamp samples with visible fractures pre-BITS testing. WC-66 tested at room temperature contains a micro-fracture along the length of core (Blue arrow point to the fracture.) WC-80 tested at 60°C with a radial fracture. WC-80 has the lowest tensile strength value (1.83MPa) out of all cores tested in this study.

A variety of unpredictable fracture patterns occurred among the 20 cores tested much like those found by Bisai and Chakraborty (2019). Figure 2.9 shows one core from each sample

group after BITS testing. No shale type and/or temperature exhibited consistent fracturing patterns. However, multiple central fractures (Figure 2.9a and b) were the most common fracturing pattern. A single "clean," central fracture, like that of WC-63, (Figure 2.9c) was the most uncommon, occurring only twice out of 20 cores. Some cores, like WC-68 (Figure 2.9d) were crushed in a non-central fashion.

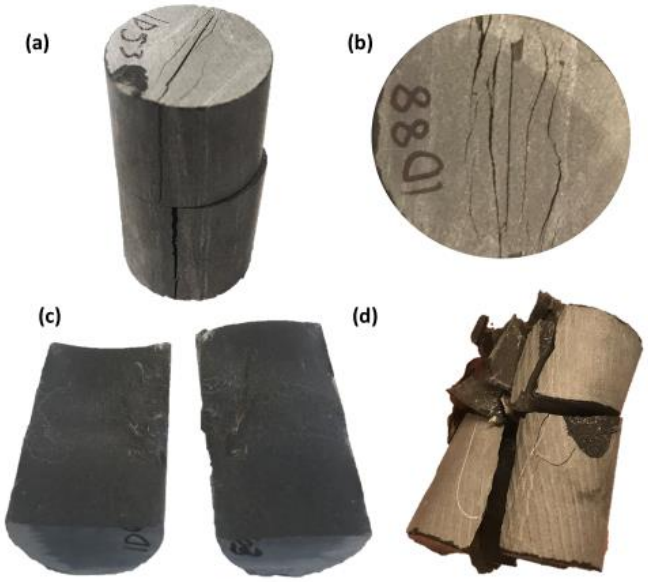

Figure 2.9. One representative core per sample group fractured in this study. (a) EF-53 tested at room temperature experienced multiple central fractures and broke in half axially. (b) The face of EF-88 tested at 60°C showcasing multiple central fractures. (c) WC-63 tested at room temperature demonstrating one "clean," central fracture. (d) WC-68 tested at 60°C had the highest tensile strength in the study at 8.52 MPa.

Temperature Effect

Results of this study record a decrease in tensile strength when temperature was increased from room temperature to 60°C for both Eagle Ford and Wolfcamp shale (although not yet statistically verified). The average tensile strength at 60°C Eagle Ford and Wolfcamp shales was reduced by 16.7% and 9.97%, respectively (Table 2.1). This finding is in opposition to the

findings of other research that found an increase in tensile strength with increased temperatures. Vishal et al. (2022) tested shale at room temperature, 50°C, 100°C, 200°C, and 400°C using BITS to determine the temperature effect on tensile strength. They concluded that there was a significant increase in average strength up to 100°C but decreased as temperatures increased past 100°C. They hypothesize the increase in values up to 100°C may be from removal of water present in the rock. However, BITS testing was not administered at temperature; their samples were heated to temperature for three hours then allowed to cool to room temperature before testing. Iferobia et al. (2022) discovered similar results to Vishal et al. (2022). They exposed samples of Eagle Ford and Wolfcamp shale to 90°C for 5 and 20 days and discovered an average tensile strength increase compared to samples tested at room temperature. They also exposed samples of Eagle Ford and Wolfcamp shale to 220°C for five days and found a decrease in average tensile strength compared to samples tested at room temperature.

Conclusions

Several conclusions can be made regarding this study:

- BITS is a preferable method to assess tensile strength over a DST method.
- Custom designed BITS test fixture produced meaningful data for the core geometry used in this study.
- Eagle Ford shale has a higher average tensile strength compared to Wolfcamp shale for cores tested at 60°C and at room temperature.
- Wolfcamp shale has more variability in tensile strength between replicates due to the existence of visible fractures resulting in a wider standard deviation in the average tensile strength of the five replicates.

- Average tensile strength is lower in cores tested at 60°C compared to cores tested at room temperature for both shale types.

Comparing tensile strength of intact shale cores at room temperature versus 60°C is the first iteration in the methods development process. Future manuscripts will include statistical analysis of results. Further studies accompanying this research will determine how mineralizing fluids effect the tensile strength of intact cores both at room temperature and 60°C using the BITS testing procedures presented here. In that study, intact cores will be saturated in a similar fashion to the cores that undergo UIPC treatment. The final goal will be to test fractured shale cores that have been sealed with UICP to compare the tensile strength of composite cores with that of intact cores to better inform geomechanical modeling.

Acknowledgements

The authors acknowledge the SubZero Science and Engineering Research facility at Montana State University for use of the X-ray μ-CT scanner and use of data processing and analysis software. The authors would like to thank the Montana State University Machining Laboratory for use of their facilities and collaboration. This study was supported by funding from the US Department of Energy, Office of Basic Earth Sciences, DOE Award No.: DE-SC0021324. Any opinions, findings, conclusions, or recommendations expressed herein are those of the authors and do not necessarily reflect the views of the Department of Energy (DOE).

CHAPTER THREE

SPLITTING TENSILE STRENGTH OF FRACTURED SHALE CORES SEALED WITH UICP

Contribution of Authors and Co-Authors

Manuscript in Chapter 3

Author: Kayla Bedey

Contributions: Experimental design, data collection, data interpretation, data analysis, writing, editing.

Author: Matthew R. Willett

Contributions: Experimental design, data collection, data analysis.

Co-Author: Dustin Crandall

Contributions: Project sponsor, editing.

Co-Author: Jonny Rutqvist

Contributions: Project sponsor, editing.

Co-Author: Kirsten Matteson

Contributions: Data interpretation, writing, editing.

Co-Author: Catherine M. Kirkland

Contributions: Experimental design, data interpretation, writing, editing.

Co-Author: Adrienne J. Phillips

Contributions: Experimental design, data interpretation, writing, editing.

Author: Al Cunningham

Contributions: Data interpretation.

Manuscript Information

Kayla Bedey, Matthew R. Willett, Dustin Crandall, Jonny Rutqvist, Kirsten Matteson, Catherine M. Kirkland, Adrienne J. Phillips, Al Cunningham

Status of Manuscript:
☒ Prepared for submission to a peer-reviewed journal
☐ Officially submitted to a peer-reviewed journal
☐ Accepted by a peer-reviewed journal
☐ Published in a peer-reviewed journal

Abstract

Fractures in subsurface shale formations are instrumental in the recovery of hydrocarbon resources. A result of hydraulic fracturing, these fractures potentially become harmful leakage passages through caprocks that may contribute undesired fluids to the atmosphere and functional groundwater aquifers. Ureolysis-induced calcium carbonate precipitation is a bio-mineralization technology that uses the urease enzyme to convert urea and calcium into calcium carbonate ($CaCO_3$) mineral deposits. The resulting bio-mineral can bridge the gaps in fractured shale and reduce fluid flow through undesired pathways. This work showcases UICP's ability to seal fractured shale cores (5.08 cm long by 2.54 cm diameter) and further investigates how UICP changes the mechanical properties of fractured shale. Two different methods were used to successfully facilitate biomineralization: 1) the flow-through method which sequentially injects UICP-promoting solutions into fractured shale cores to induce mineral precipitation and 2) the immersion method that places fractured shale cores treated with guar gum and UICP-promoting solutions into a batch reactor. This study is the first step towards determining if guar gum would be a suitable additive to UICP technology in the hopes of reducing the number of injections required to seal a fracture via flow-through methodology. Sealing methods were compared with a modified Brazilian indirect tensile strength (BITS) test to better understand how UICP and guar gum influence the mechanical properties of these composite materials. Splitting tensile strength results of this study were heterogeneous, much like the singular fractures spanning the length of each shale core. In some cores, the biomineralized fracture split apart, but notably in other cores the biomineralized fracture remained intact, demonstrating more cohesion than the surrounding shale rock.

Introduction

An abundance of natural gas (i.e., shale gas) is trapped within subsurface shale formations. Shale gas, a cleaner energy source compared to crude oil, is imperative to meeting global energy demands while the transition to economically feasible, climate-friendly alternative energy sources continues. Hydraulic fracturing (aka fracking) coupled with horizontal drilling creates a fracture network within impermeable shale allowing access to otherwise inaccessible gas resources. While this technology continues to be instrumental in the evolving energy landscape, remediating the resulting fractures is environmentally and economically advantageous.

Sealing fractures will reduce undesired leakage pathways that may lead to environmental impacts such as contaminating groundwater aquifers or methane leaking to the surface. The low permeability of shale formations makes it an excellent geologic caprock layer above those targeted for carbon sequestration. But, if caprock layers are compromised, trapped carbon dioxide (CO_2) could migrate back into the atmosphere. Furthermore, fracking recovers only a small percentage of available hydrocarbons, leaving behind excess resources in the not yet accessed rock. Economically, fracture sealing can aid in enhanced resource recovery (i.e., frack/re-frack) by extending the life and efficiency of existing and future wells.

Ureolysis-induced calcium carbonate precipitation (UICP) offers an innovative solution to seal fluid pathways in fractured shale. Unlike common fracture filling materials, like cement, UICP is advantageous because it utilizes microscopic cementing agents, low viscosity fluids, non-toxic constituents, and can penetrate microfractures.

UICP

During UICP, also known as biomineralization or bio-cementation, the hydrolysis of urea is catalyzed by the presence of the urease enzyme. When a calcium source is introduced, a calcium carbonate precipitate can form (Equation 3.1) (Kirkland et al. 2021).

$CO(NH_2)_2 + 2H_2O + Ca^{2+} \rightarrow 2NH_4^+ + CaCO_3$ (s) Equation 3.1

A wide variety of bacteria, plants, and fungi produce the urease enzyme (Krajewska, 2009; Mobley & Hausinger, 1989; Stocks-Fischer et al., 1999). This study uses the ureolytic bacteria *Sporosarcina pasteurii* because it is non-pathogenic and contains high concentrations of urease (Phillips 2013). The engineering applications of UICP are wide ranging as reviewed by Phillips et al. (2013). Subsurface application related to the work presented here include remediation related to hydraulic fracturing wells, enhanced oil and gas recovery, and improving caprock integrity for geologic carbon capture and storage (Phillips, Lauchnor, et al., 2013). Significantly, UICP has been used in field applications for plugging undesired fluid pathways in wellbore cement (Kirkland et al., 2021; Kirkland et al., 2020; Phillips et al., 2016; Phillips et al., 2018) and sandstone fractures (Cuthbert et al., 2013). Moreover, UICP can increase the compressive strength in unconsolidated, porous media like sand and soils (Cui et al., 2017; Halder et al., 2014; Montoya & DeJong, 2015; Park et al., 2014; Xiao et al., 2019; Yasuhara et al., 2012), as well as the strength of concrete building materials (Bu et al., 2018; Cheng et al., 2020). These studies show that UICP is successful in fracture sealing, permeability reduction, and geomechanical property modification.

UICP in Shale

Shale formations experience elevated temperatures and increased pressures that pose challenges to the biochemical reaction governing UICP (Equation 3.1). A few studies have explored the use of UICP in shale and successfully produced biomineral precipitation inside shale fractures while mimicking subsurface conditions. Cunningham et al. (2015) biomineralized three Opalinus shale cores, two at ambient pressure and one at a high overburden pressure, and permeability of the fractures was reduced up to four orders of magnitude. Recently, Willett et al. (2023) performed UICP at 60°C into a fractured Marcellus shale core, obtaining a drop in permeability by three orders of magnitude. Using non-invasive tools, specifically nuclear magnetic resonance (NMR) and X-ray computed tomography (CT), results of this study reveal calcite deposits bridging the gap of the fracture, creating a free-standing composite core. Another study reduced permeability in fractured shale by 3-4 orders of magnitude after UICP treatment was delivered at 60°C and 70°C (Hiebert, 2019). Remarkably, when the biomineralized shale was pulled apart, new fractures were created in the rock rather than the original fracture now biomineralized. These findings prove that UICP is capable of sealing fractures in shale rock. However, there still exists a need to investigate how a biomineral seal influences the mechanical properties of the composite UICP-shale core. This chapter explores the tensile strength of UICP and fractured shale cores to better understand the mechanical properties of these composite materials.

Splitting Tensile Strength in Shale

Tensile strength is an important mechanical property in the characterization of rock failure that assesses the ductility of a material when it is pulled apart to the point of breakage

(Dowling et al., 2019). Direct tensile strength (DTS) methods, where a specimen is pulled apart, provide the most accurate and reliable tensile results, however tests are demanding and expensive to execute (ASTM, 2008, 2016). The Brazilian indirect tensile strength (BITS) test, as outlined in Chapter 2, is commonly used in lieu of a DTS test because it is inexpensive and easy to administer (ASTM, 2016). Also referred to as the splitting tensile strength test, the procedure applies an unconfined compressive load onto a cylindrical rock specimen until it breaks, or "splits."

Numerous studies have applied the BITS methods to intact shale discs to investigate the splitting tensile strength. Fracture patterns and failure modes are documented by Bisai and Chakraborty (2019). Li et al. (2017) found different tensile behavior between Eagle Ford and Mancos shale due to differences of mineralogy, water content, pre-existing fractures, and bedding-plane orientation and laminations. Particularly, tensile strength reduces up to 66% when pre-existing microfractures are present in the shale sample, as detected via X-ray CT scanning. Furthermore, shales with lower clay content (i.e., Eagle Ford) result in higher tensile strength. The anisotropic nature of shale has been well researched with BITS testing to analyze the effects of bedding plane, lamination orientation, and/or loading orientation during time of testing (Gao et al., 2015, He & Afolagboye, 2018, Hou et al., 2018, Mokhtari et al., 2014, Simpson et al., 2014, Wang et al., 2016). Iferobia et al. (2022) tested how thermally conditioned linear fracturing fluid and elevated reservoir temperature conditions influence tensile strength of Eagle Ford and Wolfcamp shales. These studies conclude that shale type, temperature, bedding plane, water content, mineralogy, and pre-existing microfractures have an impact on the splitting tensile strength of intact shale.

Chapter Overview

The objectives of this research are twofold: 1) seal shale fractures using UICP and 2) assess the splitting tensile strength of the resulting composite biomineralized shale. The first objective looks at two different methods to facilitate UICP in fractured shale cores: flow-through and immersion. The flow-through method as outlined by Willett et al. (2023) uses the injection of UICP promoting solutions into a fractured shale core in a sequential pattern (for example 30 minutes of flow, followed by two hours of no-flow reaction period) of microbes followed by urea and calcium-containing solutions to promote mineral precipitation. The immersion method places fractured cores treated with guar gum and UICP promoting solutions in a batch reactor which is allowed to incubate over time. Guar gum is a polysaccharide, viscosity thickener used in the oil and gas industry to boost operation efficiency and reduce enhanced oil recovery costs, making it a practical additive to include in UICP treatment for subsurface applications. After cores are sealed with UICP in either the flow-through or immersion method treatment, the second objective uses a modified BITS test to compare the resulting tensile strength of biomineralized cores. Cores sealed with the flow-through method will be compared to those sealed with the immersion method. In addition, a side-by-side comparison will be provided of the strength required to break cores in their intact state versus after they are fractured and sealed with UICP. Results from this study will help to inform future geomechanical modeling efforts.

Materials and Methods

Shale Cores

Marcellus and Eagle Ford shale cores were used in this study. Marcellus shale cores were provided by the National Energy Technology Laboratory (NETL) and sourced from a vertical

well in Logan County, West Virginia (M. R. Willett et al., 2023). Eagle Ford shale cores were sourced from outcroppings of a large commercially drilled formation in Texas (Kocurek Industries, Caldwell, TX) and cored parallel to the bedding plane. All cores in this study adhere to a geometry of 2.54 cm (1 in) diameter by 5.08 cm (2 in) length. A modified Brazilian tensile strength test was used to create a single, heterogeneous fracture through the length of each core (Figure 3.1) (Bedey et al., 2023).

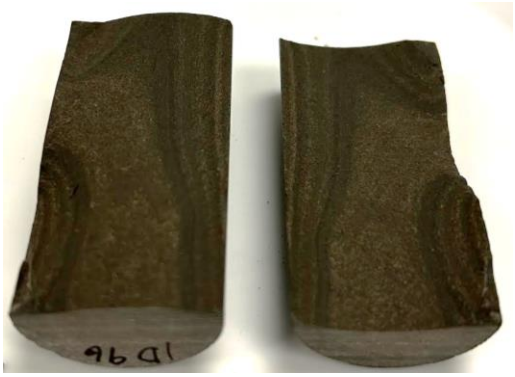

Figure 3.1. Eagle Ford shale core fractured lengthwise with a single, heterogeneous fracture.

Flow-Through Method

The flow-through sealing protocol follows that specified by Willett et al. (2023). In preparation for UICP treatment, a single, even layer of Granusil 2095 size (10/20) sand was applied to one half of the fractured shale, the other half was placed on top, and the two pieces were wrapped together with Teflon tape. Cores were housed in a braided PVC core holder that was connected to a syringe pump and placed inside an oven. Flow-through sealing experiments were conducted at 60°C. *S. pasteurii* cells were injected into the core and given a 15-minute stationary period, allowing cells to attach to the shale (although not confirmed), followed by a brine plug and finally a solution of urea and calcium. Once the urea and calcium were inside the fracture, a 2-hour stationary reaction period was allotted for biomineral promotion. Sequential

treatment cycles of *S. pasteurii* cells, brine, and calcium mineralizing media were injected into the fracture of the core until enough mineral formed to reduce the fracture permeability by three orders of magnitude. Three cores (one Eagle Ford and two Marcellus) were used with the flow through method.

Immersion Method

Four fracture treatments were evaluated during the immersion method (Figure 3.2): 1) *S. pasteurii* cells suspended in a gel solution of guar gum and a calcium mineralizing media (n = 5), 2) cells suspended in calcium mineralizing media (no guar gum) (n = 2), 3) a gel solution of guar gum mixed in calcium mineralizing media (no cells) (n = 2), and 4) a control with no cells or guar gum (n = 1). "n" refers to the number of core replicates per fracture treatment. All four conditions were tested at room temperature (RT) and 60°C, where n was mimicked per temperature. The immersion method treatment was performed on a total of 20 cores.

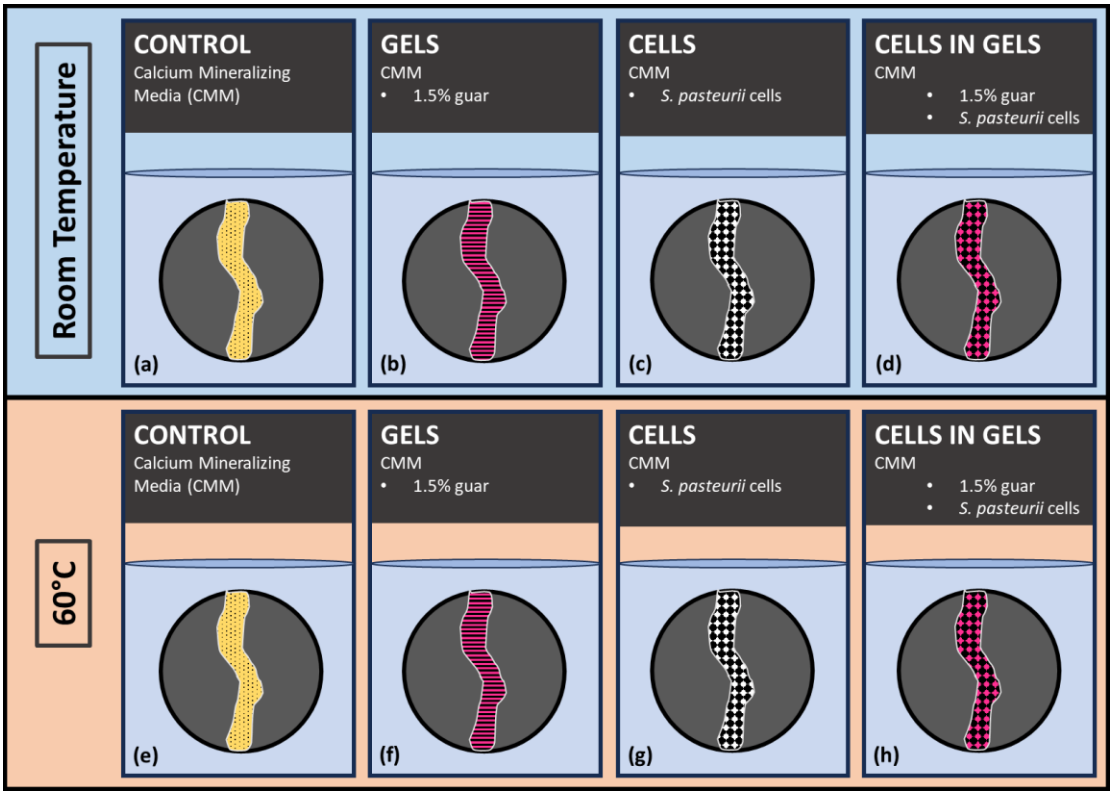

Figure 3.2. Four fracture treatments were investigated with the immersion method. All conditions use calcium mineralizing media (CMM) as a base fracture filling fluid. (a and e) The "control" treatment assessed the CMM's ability to seal fractures (number of replicates (n) = 1). (b and f) The "gel" treatment incorporated a 1.5% guar gum concentration into the CMM to enhance viscosity and determine if guar gum influences core sealing (n = 2). (c and g) The "cell" treatment integrated a high concentration of *S. pasteurii* cells (OD > 1.8) into the CMM fluid to promote mineral precipitation inside the fracture. (d and h) The "cells in gels" condition combined 1.5% guar gum and highly concentrated *S. pasteurii* cells (OD > 1.8) into the CMM (n = 5). All treatments were immersed in a urea and calcium solution. Sealing was attempted at room temperature and 60°C for each condition where number of replicates was mimicked per temperature (i.e., n = 5 for "cells and gels" condition at room temperature and n = 5 for "cells in gels" treatment at 60°C for a total of 10 cores).

All mixtures utilized calcium mineralizing media (CMM) as a base fracture filler fluid. The "control" treatment was simply CMM consisting of 35 g/L sodium chloride, 1 g/L ammonium chloride, 3 g/L nutrient broth, and 40 g/L urea; a pH adjustment between 6.0-6.3; then adding 96 g/L calcium chloride dihydrate. Fracture treatments that integrated guar gum, or "gels," were produced when 0.75 g guar gum was added to 50 mL of CMM, creating a 1.5%

guar solution. The intention of the "gels" treatment was to determine if the guar gum was capable of sealing fractures without the influence of mineral precipitation. "Cells in gels" was the only fracture treatment to contain both *S. pasteurii* cells and guar gum in the CMM base fluid.

Fracture treatments containing "cells" incorporated an *S. pasteurii* culture into the CMM base fluid. Cell preparation began when 100 mL of brain heart infusion (37 g/L), amended with 2% urea (20 g/L), was inoculated with 1 mL of thawed *S. pasteurii* (ATCC 11859) frozen stock culture, and placed in a 30°C incubator at 150 rpm. After incubating for 24 hours, 2 mL of the culture was transferred into 200 mL of yeast extract (YE) media and placed in a 30°C incubator at 150 rpm. YE media was made using 15.5 g/L yeast extract, 35 g/L sodium chloride, 1 g/L ammonium chloride, and 20 g/L urea. Following a 16-hour incubation period, the transfer culture was spun down using a Thermo Scientific Sorvall Legend XTR Centrifuge at 2964xg for 10 minutes at 4°C. The bacterial pellets were resuspended in 50 mL of CMM. 200 µL of resuspended culture was injected into a Greiner Bio-One 96 well plate, and the bacteria concentration was assessed using a Tecan Infinite F50 absorbance reader with a 600 nm filter, where the optical density at 600 nm was >1.8.

Approximately 3 mL of fracture filler was applied to the fractured faces of each core. After the CMM and/or cell and/or gel fracture treatment was applied to the shale fracture, 0.5 g of Granusil 2095 size (10/20) sand (~1 mm in diameter) was evenly added in one layer to one half of the fractured core. The other half was placed on top, the two pieces were sandwiched together, and ½ inch Teflon tape was wrapped around the center of the core to prevent displacement of the fractured halves. The cores and fracture filler sandwich were then allotted a 30 min attachment period. Cores designated for sealing at 60°C were placed inside an oven

preheated and conditioned to 60°C for the duration of their attachment period. Cores selected for sealing at RT were left at RT for their attachment period.

Cores were then immersed in a urea and calcium (U+C) solution for 48 hours to promote mineral precipitation. U + C was made by combining 35 g/L sodium chloride, 1 g/L ammonium chloride, and 20 g/L urea; adjusting pH to 6.0-6.3; and subsequently adding 48 g/L calcium chloride dihydrate. Cores designated for sealing at 60°C were placed inside an oven preheated to 60°C for the duration of their 4-hour immersion reaction period. Those at RT were left at RT for their immersion reaction period. After the reaction period, cores were removed from their beakers and placed in a 40°C incubator to dry for five days. Cores mass was weighed over the five-day period until mass remained stable. Once dry, the Teflon tape wrapped around the center of the core was removed and cores were inspected for sealing. Figure 3.3 depicts the immersion method steps.

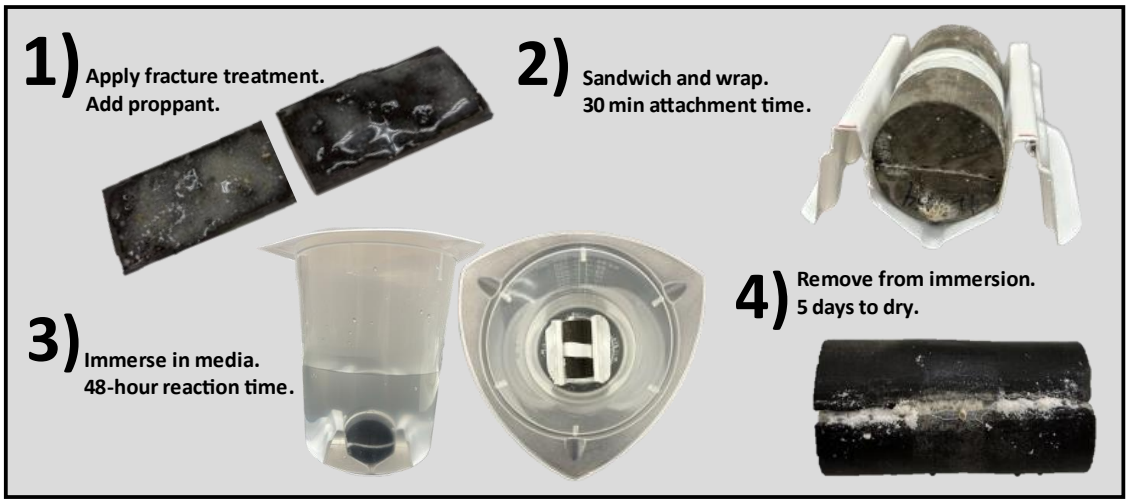

Figure 3.3. Immersion Method. 1) Apply ~3 mL fracture filler to fracture faces and sprinkle with 0.5 g proppant. 2) Sandwich cores halves together and wrap 1/2-inch Teflon tape around center of core. Let sit at the designated temperature; room temperature or 60°C; for 30 minutes. 3) Immerse into U+C media, at designated temperature, for 48 hours. 4) Remove from immersion after 48 hours and place in 40°C incubator to dry for five days. After five days, take out of incubator, remove Teflon tape, and inspect for sealing. Sealing is successful when the two core halves are attached to one another without the aid of tape.

Tensile Strength

A modified Brazilian indirect tensile strength (BITS) test was used to evaluate the splitting tensile strength of the sealed cores. Methods paralleled those used on intact shale cores (5.08 cm long by 2.54 cm diameter) as described by Bedey et al. (2023). Tests were administered on an MTS Criterion Model 43 test frame enclosed in an environmental chamber that allows testing at elevated temperatures. Testing was completed with a 30 kN load cell and the cutoff load was set to 28 kN. Curved platens were designed to accommodate the geometry of the cores in this study and fabricated to connect with the test frame. Splitting tensile strength was calculated using Equation 3.2:

$$\sigma_t = 1.272P / \pi tD \qquad \text{Equation 3.2}$$

Where σ_t is the splitting tensile strength (MPa or psi), 1.272 is a coefficient when curved platens are used, P is the maximum applied load indicated by the testing machine (N or lbf), t is the thickness of the specimen (mm or in), and D is the diameter of the specimen (mm or in) (ASTM 2016). Equation 3.2 is specific to BITS tests utilizing curved loading platens, as indicated by the coefficient 1.272. Curved loading platens are used on the cores in this study to reduce the stress concentration at the loading points (ASTM, 2016; Mellor & Hawkes, 1971). Tensile strength per core was evaluated at the temperature used to seal the core, either room temperature or 60°C (i.e., cores sealed at 60°C were tested at 60°C). Cores tested at 60°C were placed inside the environmental chamber for a 3-hour equilibration period prior to testing.

Results and Discussion

Prior to sealing, a single heterogeneous fracture was induced along the length (5.08 cm) of each intact shale core using a modified BITS test (Bedey et al., 2023). The average compressive load applied to the intact Eagle Ford shale cores (n = 20) was 17.59 ± 2.26 kN, resulting in a splitting tensile strength of 5.52 ± 0.71 MPa. Loads applied to the two Marcellus cores were not made available to this project as they were split by collaborators at NETL prior to shipment to Montana State University.

The flow-through method sealed three shale cores (two Marcellus and one Eagle Ford) with biomineralization (Figure 3.4). Each core received between 20-30 injections of UICP treatment until permeability in the fracture reduced by three orders of magnitude. Once removed from their core holders, cores that were once two pieces of shale were connected and held together with biomineralization, similar to what has been seen in previous UICP-shale research (Cunningham et al., 2015; Hiebert, 2019; M.R. Willett et al., 2023). Both Marcellus cores, M-29

and M-32, were sealed along their entire length, creating a 5.08 cm long composite core (Figure 3.4a and b). However, EF-48, the Eagle Ford core, suffered a secondary fracture during UICP treatment while inside the core holder, likely due to hose clamps applying an overburden pressure to the core, causing it to split axially into two halves of approximately equal size, around 1 inch each (Figure 3.4c). The half of the core closest to the influent of fluids was successfully sealed together with biomineralization whereas the half near the effluent was not connected. The approximate 1-inch sealed half of EF-48, along with M-29 and M-32, were tested for mechanical strength.

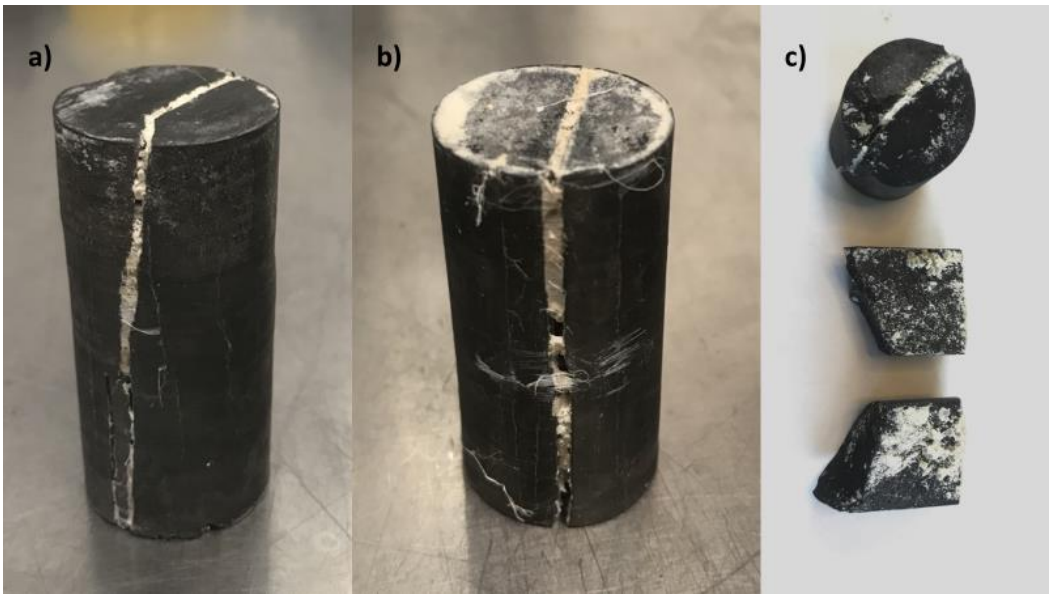

Figure 3.4. Shale cores sealed with UICP technology using the flow-through method. (a) Marcellus shale core, M-29. (b) Marcellus shale core, M-32. (c) Eagle Ford shale core, EF-48, suffered a secondary fracture during UICP treatment while inside core holder, causing it to split in two 1-inch halves along its length. The half of the core closest to the fluid influent sealed with biomineralization and the half near the effluent did not seal. Fully sealed and partially sealed cores were tested for mechanical strength.

Flow-through cores experienced multiple breaks before experiencing a definitive maximum failure event. Table 3.1 displays the maximum compressive load as well as the calculated splitting tensile strength each core experienced during their respective BITS test.

Table 3.1 Flow-through method maximum compressive load applied to core and the calculated splitting tensile strength results. *EF-48 broke axially into 2 halves during UICIP treatment. Only ½ of the core sealed and was mechanically tested.

Core ID	Compressive Load (kN)	Splitting Tensile Strength (MPa)
M-29	5.26	1.71
M-32	9.82	3.20
EF-48*	13.71	4.46
Average	9.60 ± 4.23	3.12 ± 1.38

The immersion method sealed fourteen of the twenty Eagle Ford shale cores, with success being found in treatments utilizing guar gum. Here, successful sealing is defined when the applied fracture treatment allowed cores that were once two pieces to become one composite free-standing core. Cores using the “cells” (*S. pasteurii* culture in CMM base fluid) and “control” (CMM base fluid) fracture treatments did not seal under either temperature condition (Fig 3.5). Cores that did not seal (six total) maintained their original fractured condition and were not mechanically tested. The strength of the fracture treatment could not be evaluated. A tensile strength of 0 MPa was assumed for unsealed cores.

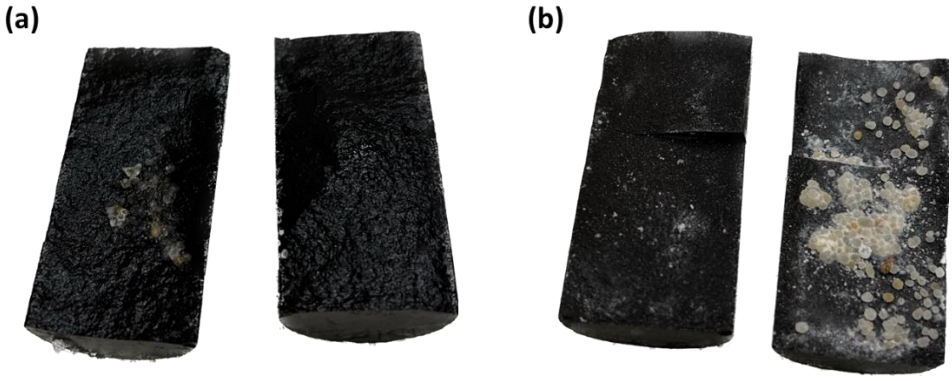

Figure 3.5. Representative unsealed cores from “control” and “cells” only fracture treatments. (a) EF-102 using the “control” fracture treatment. No cells or gels were used in this treatment, resulting in no mineral precipitation and no sealed cores. (b) EF-108 using the “cells” only fracture treatment. There is evidence of mineral formation, but no cores were able to seal using this treatment.

The “gels” and “cells in gels” fracture treatments experienced 100% success rate in sealing cores under both temperature conditions, for a total of 14 sealed cores (Figure 3.6). These results demonstrate that guar gum positively influences core sealing. Although approximately the same quantity of microbes was applied to cores under the “cells” and “cells in gels” fracture treatments, the “cells in gels” cores likely exhibited sealing success because the cells were suspended in a higher viscosity guar gum fluid, allowing microbes to remain inside the fracture for the sealing process. When only “cells” were applied as a fracture treatment, the treatment had difficulty staying inside the fracture to induce mineral precipitation. Figure 3.5b shows evidence of mineral precipitation attaching pieces of proppant to each other as well as the shale rock; however, mineral was not sufficient to attach the shale halves to one another. All sealed cores were mechanically tested using a modified BITS method (Bedey et al., 2023).

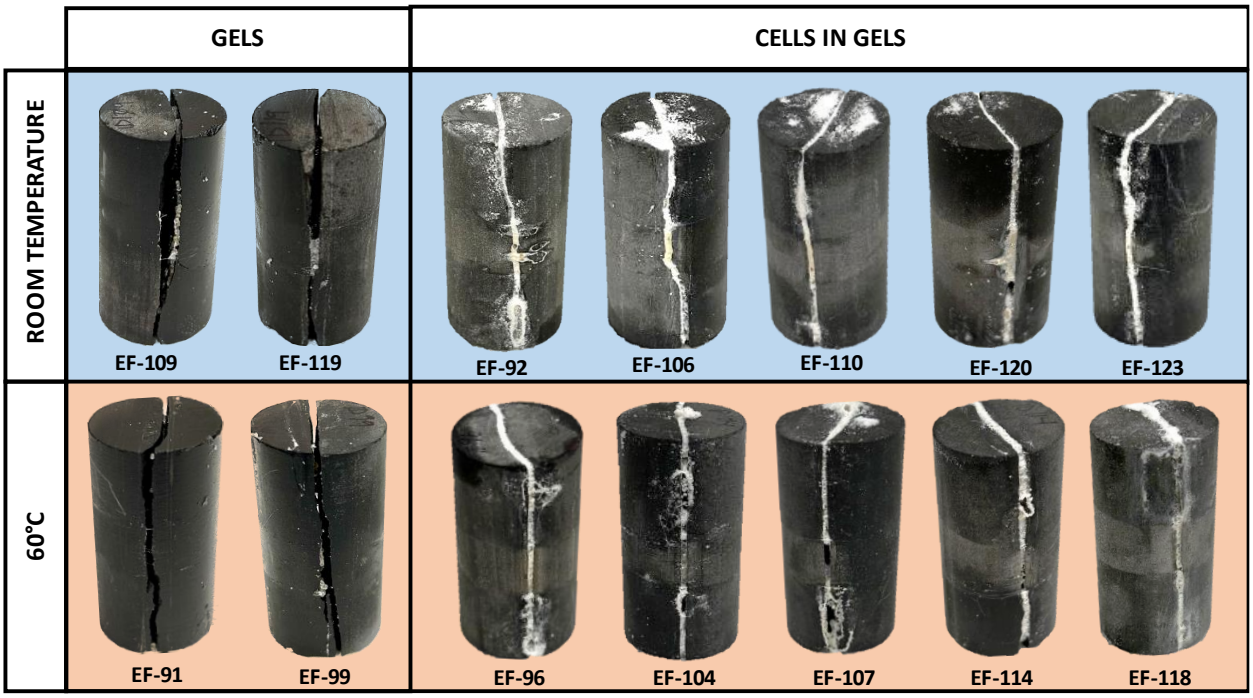

Figure 3.6. Cores sealed using the immersion method. Four cores (two at room temperature and two at 60°C) sealed using the "gels" fracture treatment that contained guar gum and UICP promoting fluids (no cells). Ten cores (five at room temperature and five at 60°C) sealed using the "cells in gels" fracture treatment that contained cells, guar gum, and UICP promoting fluids.

Cores under the "gels" only fracture treatment demonstrated two distinct results. Cores at RT conditions (EF-109 and EF-119) maintained fracture cohesion with guar gum during and after tensile testing (Figure 3.7a), compared to those sealed and tested at 60°C (EF-99 and EF-119) which experienced fracture treatment failure (Figure 3.7b). The load-displacement curves for gel treated cores (Figure 3.8) indicate distinct failure episodes occurring between 20-27 kN. These results suggest further research may be necessary to determine the impact guar gum plays as an additive to UICP technology. Due to a small sample size (n = 2 per temperature condition) it is difficult to draw distinct conclusions and additional testing should be considered.

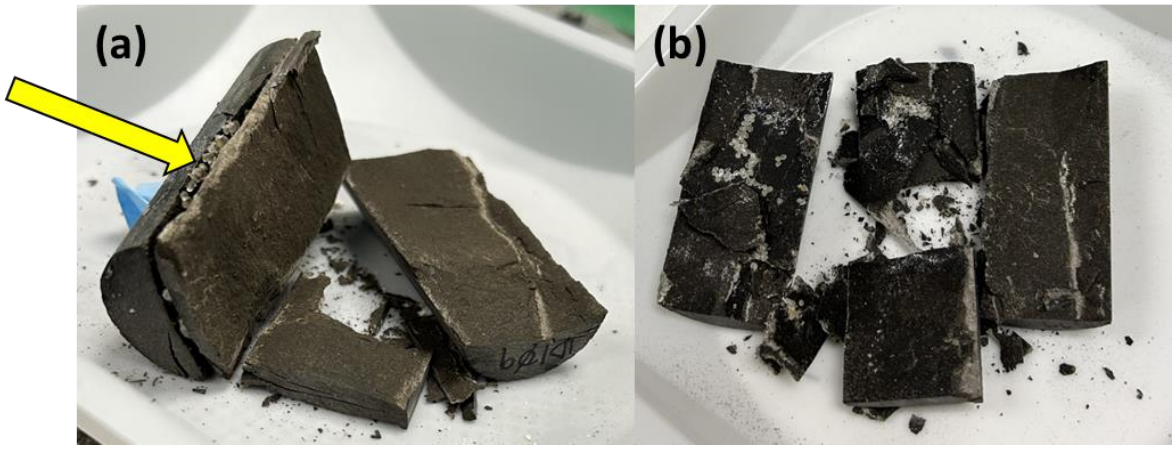

Figure 3.7. Representative cores sealed using the immersion method with the "gels" fracture treatment. (a) EF-109 sealed at room temperature. The yellow arrow points to the original fracture maintaining cohesion with guar gum. (b) EF-99 at 60°C where the guar gum seal failed.

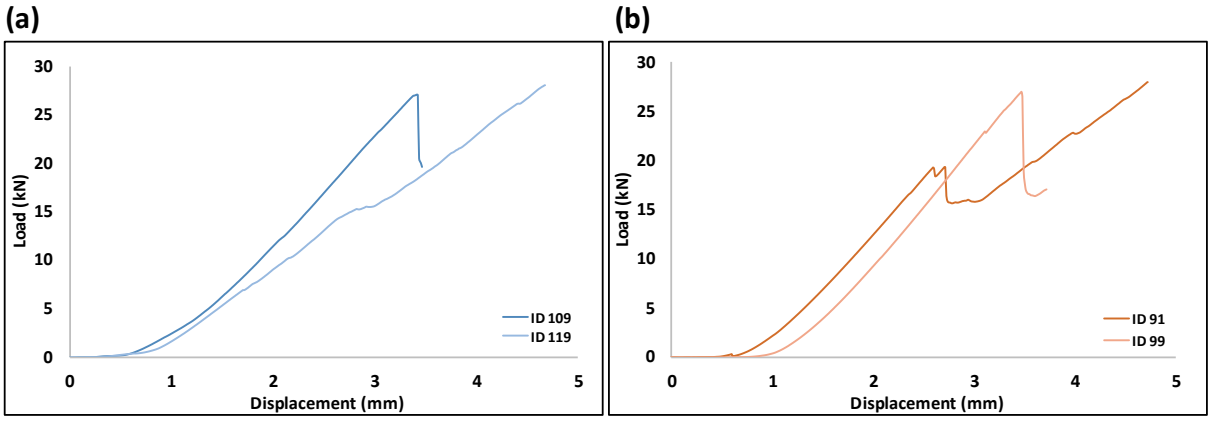

Figure 3.8. "Gels" fracture treatment load (kN) vs displacement (mm) curves. (a) Room temperature cores. (b) 60°C cores.

Multiple breaks were observed in cores sealed using the immersion method (Figure 3.8 and 3.9). Table 3.2 reports the significant failure episodes for sealed cores treated with guar gum, cells, and UICP promoting solutions. Cores using this fracture treatment experienced their first indication of failure at an average compressive load of 0.66 ± 0.19 kN (average splitting tensile strength = 0.21 ± 0.06 MPa) and 0.55 ± 0.07 kN (average splitting tensile strength = 0.17 ± 0.02 MPa) when tested at RT and 60°C, respectively (Table 3.2 and Figure 3.9). Out of the 10 total

composite cores, three (EF 110 and EF-123 at RT and EF-96 at 60°C) experienced failure in the mineralized fracture at the first indication of failure, at a load <1 kN, and the test ended immediately. When removed from the testing apparatus, these cores were split apart at the mineralized fracture. Although the other seven composite cores also experienced a break at a load < 1 kN, complete capacity was not lost and the test was able to continue, incurring further breakage.

Table 3.2. Failure episodes for cores sealed with the immersion method using the cells and guar gum fracture treatment (i.e., "cells in gels") as determined with BITS testing methods. Failure for each episode is reported in compressive load, C (kN), and the calculated tensile strength, σ_t (MPa), using Equation 3.2.

		1st Failure		2nd Failure		3rd Failure		4th Failure		Load Cell Limit	
T	Core ID	C (kN)	σ_t (MPa)	C	σ_t	C	σ_t	C	σ_t	C	σ_t
RoomTemp	EF-92	0.97	0.31	17.58	5.52	23.53	7.38	-	-	28.03	8.80
	EF-106	0.66	0.21	6.67	2.09	-	-	-	-	-	-
	EF-110	0.63	0.20	-	-	-	-	-	-	-	-
	EF-120	0.46	0.15	13.38	4.20	-	-	-	-	28.04	8.80
	EF-123	0.56	0.17	-	-	-	-	-	-	-	-
60°C	EF-96	0.48	0.15	-	-	-	-	-	-	-	-
	EF-104	0.49	0.15	14.63	4.59	24.12	7.57	-	-	28.05	8.80
	EF-107	0.59	0.19	0.84	0.26	22.38	7.02	25.31	7.94	28.03	8.80
	EF-114	0.52	0.16	16.58	5.20	-	-	-	-	28.06	8.80
	EF-118	0.64	0.20	19.91	6.25	-	-	-	-	28.02	8.80

At 60°C, cores EF-104, EF-107, EF-114, and EF-118 suffered a significant second (third or fourth) failure episode in the range of 15 – 25 kN (Table 3.2 and Figure 3.9b). This was also seen in EF-92 at RT (Figure 3.9a). However, EF-106 and EF-120 did not show a similar trend. EF-106 experienced a second break much sooner at 6.67 kN and the test ended. EF-120 experienced a minor failure episode at 13.38 kN but the test ended only when the load cell reached its load limit of 28 kN. Both cores broke at the mineralized fracture. Notably, four cores

at 60°C and two cores at RT experienced a test that ended when the load cell reached its limit cutoff load of 28 kN. These tests would have continued if the load cell was to apply a higher load. Upon removing cores from the apparatus, visible fractures in the shale rock matrix were evident. Of the four 60°C cores, three (EF-104, EF-114, and EF-118) maintained mineral cohesion and exhibited new fractures in the surrounding shale rock; as did one of the RT cores (EF-92). Mineral cohesion means that the biomineral sealing the fracture together did not experience enough failure to break apart. These results may indicate that the load cell used in the testing apparatus is not strong enough to test the full capacity of a biomineralized seal.

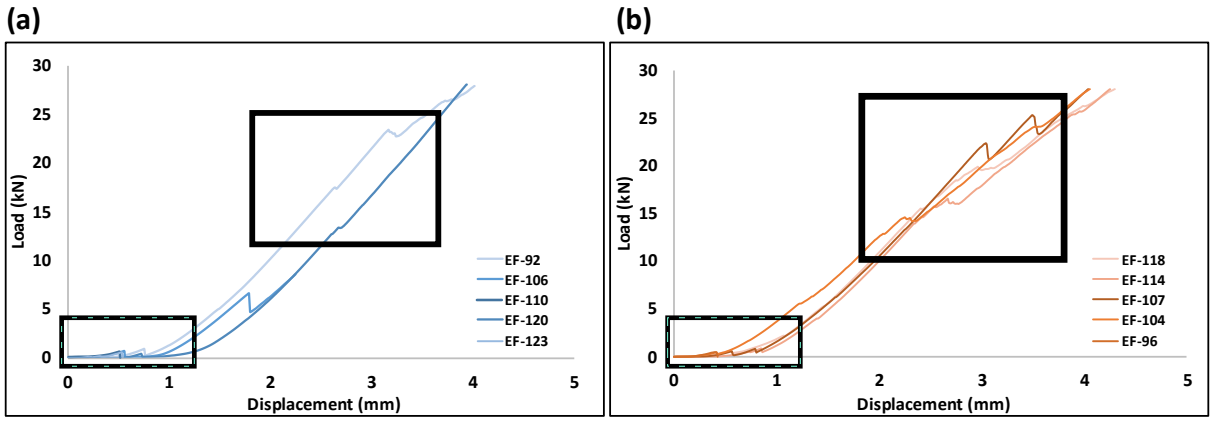

Figure 3.9. "Cells in gels" fracture treatment load (kN) vs. displacement (mm) curves. The small, checkered box shows the first indication of failure. The large black box highlights the second and/or third failure episode. (a) Room temperature cores. (b) 60°C cores.

Regardless of sealing method, results on how and where each biomineralized core broke were unpredictable (Figure 3.10 and 3.11). The load (kN) versus displacement (mm) curves for cores sealed with the flow-through method compared to those sealed with the immersion method show visual differences in how the composite cores reacted to BITS testing (Figure 3.10). Figure 3.10a showcases the variety of failure episodes experienced by cores sealed with the flow-through method (n = 3). The maximum load incurred by a flow-through core was 13.71 kN

(tensile strength = 4.46 MPa) as seen by EF-48. In contrast, cores sealed with the immersion method exhibited fewer failure episodes (one – four episodes per core) and failure trends were similar between temperature conditions (Figure 3.10 b and c). Differences in the failure behavior may be attributed to the UICP sealing methods. Cores sealed with the flow-through method were subjected to more rigorous handling in which they were saturated in UICP promoting fluids at 60°C for seven to ten days, received 20 – 30 bacterial applications, experienced overburden pressure from the reactor core holder design, and subject to NMR and CT analysis before and after UICP treatment. The authors hypothesize that these more rigorous methods may have influenced the shale rock matrix but acknowledge that more experimentation needs to be done to draw any conclusions. Comparatively, cores sealed with biomineral using the immersion method were saturated in UICP promoting fluids for two days (five at room temperature and five at 60°C), received one bacterial application, and experienced no overburden pressure during the immersion process; however, they did have guar gum incorporated into UICP promoting fluids. Nevertheless, the unpredictability of core breakage remains, making it difficult to draw comparisons between UICP treatment methodology. In some cases, the mineralized fracture remained intact showing more cohesion than the surrounding shale rock, similar to what was seen in the work by Heibert (2019). In other cases, the biomineralized fracture experienced mineral failure and broke open from an insufficient seal. Of the three cores sealed with the flow-through method, two experienced mineral cohesion and one mineralized fracture split apart during the BITS test (Figure 3.11a). Cores sealed at 60°C using the cells in gels fracture treatment had better mineral cohesion success than those at RT. 60% of 60°C cores (n = 5) experienced mineral cohesion compared to only 20% at RT (n = 5) (Figure 3.11 b and c).

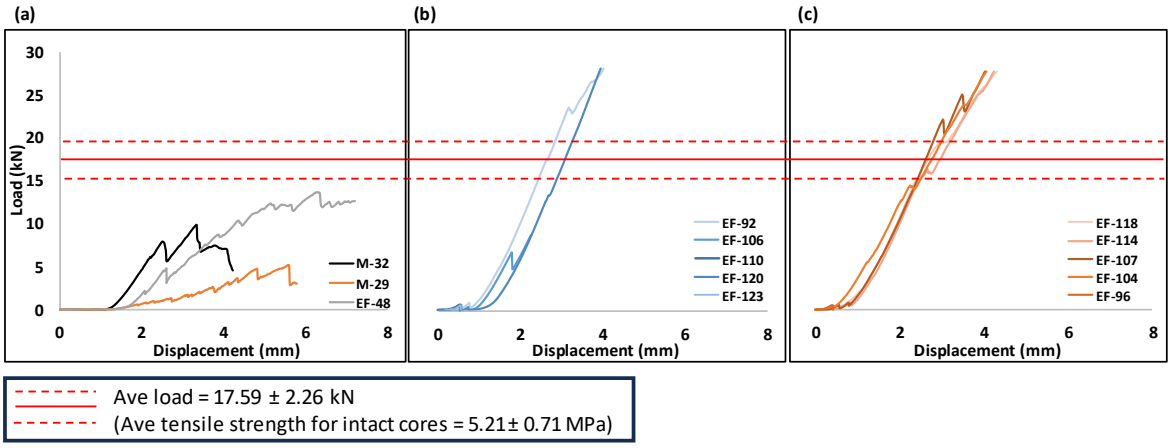

Figure 3.10. Load (kN) vs. displacement (mm) curves for all cores sealed with UICP. The solid red line indicates the average load (kN) required to break the intact Eagle Ford shale cores (n = 20) prior to sealing with the immersion method and the dashed red lines indicate the standard deviation associated with the average. (a) Curves for cores sealed with the flow-through method at 60°C. (b) Curves for cores sealed with the immersion method at room temperature. (c) Curves for cores sealed with the immersion method at 60°C. Cores sealed with the immersion method utilized cells, guar gum, and UICP promoting solutions in the “cells in gels” fracture treatment.

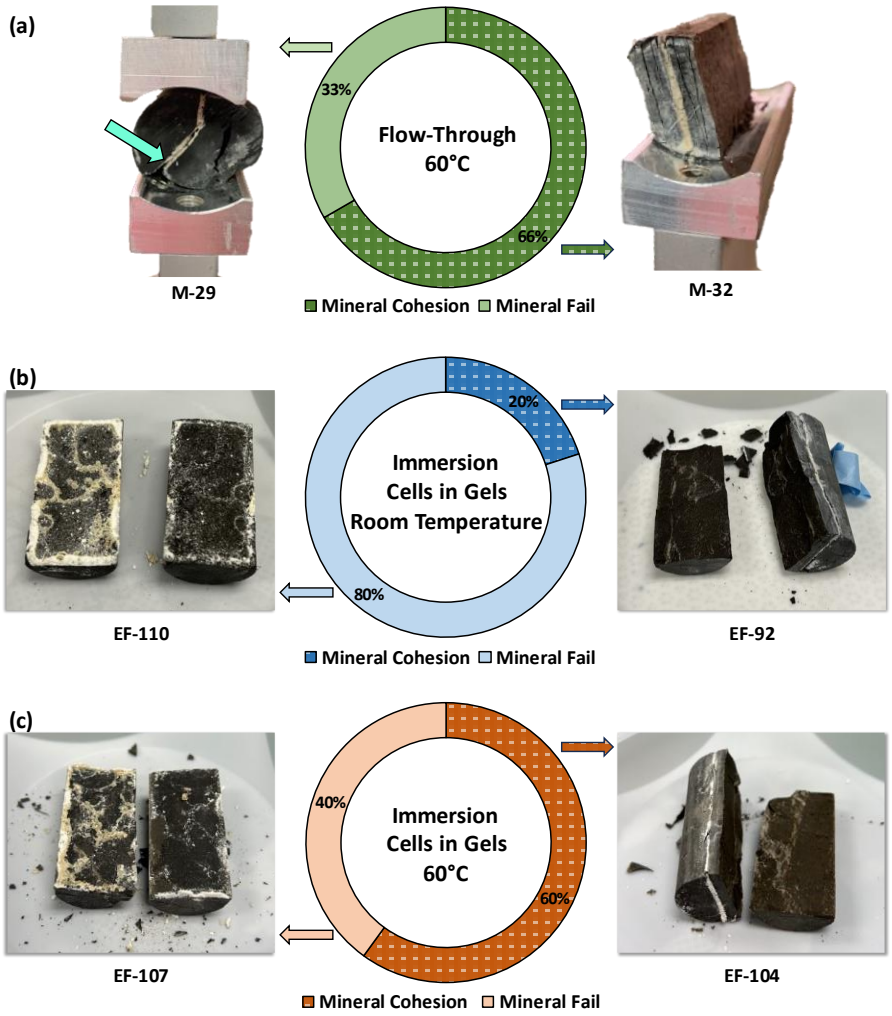

Figure 3.11. Pie charts showcasing the percentage of mineral cohesion (dark color) versus mineral failure (light color) post BITS testing for cores sealed with UICP. (a) The flow-through method at 60°C. Three cores were sealed and tested at 60°C, where one (M-29) experienced mineral failure during testing and two maintained mineral cohesion during and after testing, like the representative core M-32. The blue arrow points to a fractured mineral seal on M-29. (b) The immersion method at room temperature. Five cores were sealed and tested at room temperature, where four experienced mineral failure during testing, like representative core EF-110, and one (EF-92) maintained mineral cohesion during and after testing. (c) The immersion method at 60°C. Five cores were sealed and tested at 60°C, where two experienced mineral failure during testing, like representative core EF-107, and three maintained mineral cohesion during and after testing, like the representative core EF-104.

While it is difficult to predict how the cores would break, several causes of heterogeneity in the composite cores could be the reason. The authors hypothesize that the UICP promoting

fluids used here could cause changes in the rock matrix, although this is not yet confirmed. Shale by nature is anisotropic and highly variable between shale types which could lead to uncertainties and compromises (pre-existing fractures) in the core rock matrix. The lithology and mineral content of different shale types may influence how the cores broke. Figure 3.12 shows the average mineral content (percentage of carbonates, silicates, and clay) for shales used in this study (Eagle Ford and Marcellus) and those used by Bedey et. al (2023) in developing BITS testing methods (Eagle Ford and Wolfcamp). Notably, the average mineral content per shale type is highly variable and may influence the strength of the rock core matrix. Additionally, the single fracture along the length of the core was induced to be heterogeneous to reflect fractures that might occur in the subsurface via hydraulic fracturing. The heterogeneity of the lengthwise fracture influences where biomineral may form inside the fracture, in turn increasing the heterogeneity to the BITS testing. Furthermore, the formation of biomineral is not homogenous inside fractures. Willett et al. (2023) uses NMR and CT to show how biomineral preferentially formed on and around pieces of proppant inside a UICP treated shale core. They show it is nearly impossible to evenly distribute proppant and have it maintain its location within a fracture which led to uneven mineral formation throughout the fracture aperture.

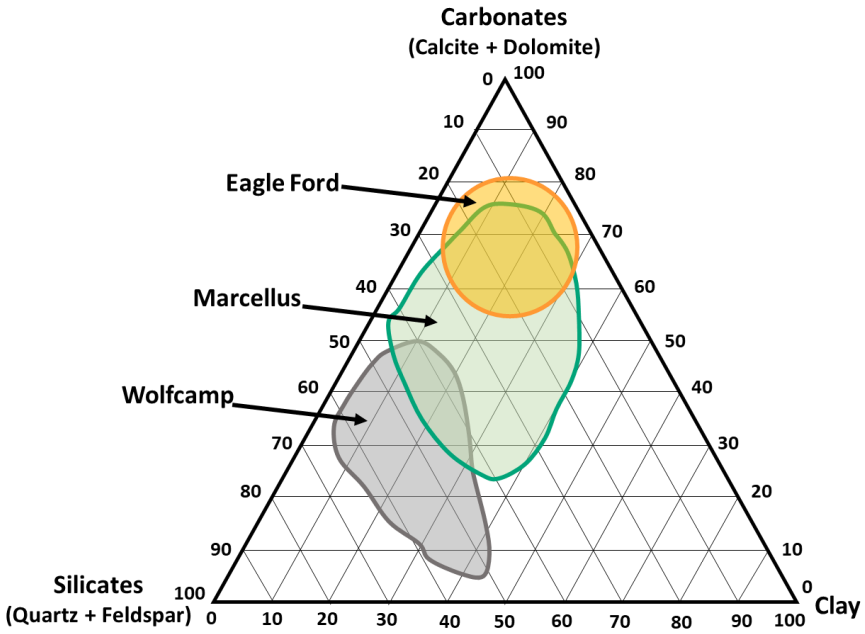

Figure 3.12. Ternary diagram showing average mineral content for shales used in this study (Eagle Ford and Marcellus), as well as shales used by Bedey et. al (2023) to develop BITS testing methods (Eagle Ford and Wolfcamp). Diagram modified from Mews et. al (2019).

Moreover, cores sealed with the immersion method received one application of highly concentrated bacterial treatment (optical density at 600 nm was >1.8), whereas flow-through cores received 20 – 30 sequential bacterial injections with an optical density at 600 nm >0.6. Population assays of the two different bacterial concentrations have not been done to date, but the authors recognize the importance of performing this work. Highly concentrated bacterial treatments may not be appropriate for flow-through methods as the end of the core closest to the injection point notoriously experiences a decrease in permeability before other places in the fracture aperture. Rapid permeability reduction at the fracture influent is observed in other UICP treated fractured rock studies such as sealing fractured shale cores (Willett et al., 2023), fractured granite cores (Tobler et al., 2018), and fractured anhydrite with gouges (Sang et. al., 2022). Increased bacterial concentrations may contribute to influent clogging phenomena causing a

rapid decrease in fracture permeability without necessarily producing enough mineral deposits to hold the shale together.

Conclusions

Several conclusions can be made regarding this study:

- Shale cores can be sealed using a variety of UICP treatment delivery methods: flow-through and immersion method.
- Not all immersion method fracture treatments ("cells" and "controls") were capable of sealing shale cores.
- Immersion method fractured treatments that included guar gum ("gels" and "cells in gels") experienced a 100% sealing success rate at room temperature and 60°C.
- Cores experienced multiple breaks during Brazilian indirect tensile strength (BITS) testing.
- Cores sealed at room temperature with guar gum ("gels" fracture treatment) showed fracture treatment cohesion after BITS testing whereas those sealed with guar gum at 60°C did not.
- Cores sealed with UICP and tested at 60°C (under either flow-through and immersion method) exhibited more mineral cohesion after mechanical testing than cores sealed and tested at room temperature (under immersion method).

Using the current flow through methodology (Willett et al., 2023) to seal shale fractures is tedious. The deployment of 20 – 30 injection cycles is lengthy and would add cost to field application. The immersion method was used to assess which fracture treatments should be

pursued for additional flow through experiments. This work shows that guar gum is a suitable additive to UICP solutions, intended to increase efficiency of flow-through treatment and reduce the number of injections required to reduce fracture permeability and seal fractured core. Recommended future research may involve adding guar gum into UICP promoting medias used for the flow-through sealing protocol. Additional studies could include testing the strength of biomineral on its own and investigating the strength contribution of guar gum in fracture sealing.

Acknowledgements

The authors acknowledge the SubZero Science and Engineering Research facility at Montana State University for use of the MTS Criterion Model 43 testing apparatus. The authors would like to thank the Montana State University Machining Laboratory for use of their facilities and collaboration. This study was supported by funding from the US Department of Energy, Office of Basic Earth Sciences, DOE Award No.: DE-SC0021324. Any opinions, findings, conclusions, or recommendations expressed herein are those of the authors and do not necessarily reflect the views of the Department of Energy (DOE).

CHAPTER FOUR

CONCLUSION

In Chapter two, methods were developed to fracture intact shale cores (5.08 cm long by 2.54 cm diameter) using a modified Brazilian indirect tensile strength (BITS) test, also known as a splitting tensile strength test. Two varieties of shale, Eagle Ford and Wolfcamp, were tested in this chapter at both room temperature and 60°C. A total of 20 cores were tested in this study under 4 testing conditions: Eagle Ford at room temperature (n = 5), Eagle at 60°C (n = 5), Wolfcamp at room temperature (n = 5), and Wolfcamp at 60°C (n = 5). A statistical analysis of the findings in Chapter two was completed after its original publication. Statistical methods can be found in Appendix A. It was hypothesized that tensile strength would be influenced by shale type and the temperature with which cores were tested. Specifically, (1) that cores tested at room temperature would exhibit a higher mean tensile strength than those at 60°C, and (2) the mean tensile strength would be different for shale types. The first hypothesis was confirmed in Eagle Ford cores (one-sided p-value = 0.0043), however Wolfcamp cores showed no evidence (one-sided p-value = 0.3198) of a difference of mean tensile strength between the temperature conditions. Although Wolfcamp cores experienced an overall greater variability in tensile strength values compared to Eagle Ford, the second hypothesis was contradicted with no evidence in the difference of mean tensile strength values between shale types (two-sided p-value = 0.2064). However, the author recognizes that the statistical differences between testing conditions are difficult to establish due to the small number of replicates in each shale type and temperature testing condition. Methods developed and results from Chapter two were used to inform mechanical testing of fractured and sealed cores in Chapter three.

Chapter three showcases UICP's ability to seal shale cores (5.08 cm long by 2.54 cm diameter) with a single heterogeneous fracture spanning the length of the core. UICP successfully sealed cores via two methods: 1) the flow-through method and 2) the immersion method. The flow-through method sequentially injects UICP-promoting solutions into fractured shale cores to induce biomineralization. A range of 20 – 30 injections was found to seal cores and reduce fracture permeability by three orders of magnitude. The immersion method determined guar gum to be a suitable additive to UICP technology, with the hope of reducing the number of injections necessary to seal cores with the flow-through method. Here, fractured shale cores treated with guar gum and UICP promoting solutions were placed into a batch reactor and allowed to incubate for an allotted time. The modified BITS methods established in Chapter two were used to evaluate the tensile strength of the sealed UICP-shale composite cores to better understand how UICP and guar gum influence the mechanical properties of these composite materials. Sealed cores experienced a mixture of tensile results indicating no clear trends. However, notably, many cores exhibited more cohesion in the mineralized fracture than the surrounding shale rock during and after mechanical testing, confirmed by the observed failure modes.

The research presented in this thesis provides evidence that UICP treatment can seal heterogeneous fractures in shale rock. Results from this thesis will inform future geomechanical modeling efforts.

Future Directions

Future work should further investigate guar gum as an additive to UICP treatment. This could involve performing flow-through sealing experiments where guar gum is added to UICP

promoting fluids and an exploration on the strength contribution of guar gum is performed. Future studies should include sealing cores from a wider variety of commonly fracked, hydrocarbon rich shale formations to assess if UICP is compatible with other shale lithologies. Finally, additional research into UICP's sealing capabilities under extreme subsurface conditions (i.e., overburden pressure and higher temperature) should be investigated before field application.

REFERENCES CITED

Achal, V., Mukherjee, A., Kumari, D., & Zhang, Q. Z. (2015). Biomineralization for sustainable construction - A review of processes and applications. *Earth-Science Reviews*, *148*, 1-17. https://doi.org/10.1016/j.earscirev.2015.05.008

Akyel, A. (2022). *Improving pH and Temperature Stability of Urease for Ureolysis-Induced Calcium Carbonate Precipitation* [Dissertation, Montana State University]. Bozeman, Montana.

ASTM. (2008). D2936-20 Standard Test Method for Direct Tensile Strength of Intact Rock Core Specimens. In. West Conshohocken, PA, USA: ASTM International.

ASTM. (2016). D3967-08 Standard test method for splitting tensile strength of intact rock core specimens. In. West Conshohocken, PA, USA: ASTM International.

Bedey, K., Cunningham, A. B., Phillips, A. J., Kirkland, C. M., Willett, M. R., Dobeck, L., Eldring, J., Crandall, D., & Rutqvist, J. (2023). Developing Methods to Assess Changes in Mechanical Properties of Shale Modified by Engineered Mineral Precipitation. 57th U.S. Rock Mechanics/Geomechanics Symposium,

Bisai, R., & Chakraborty, S. (2019). Different Failure Modes of Sandstone and Shale under Brazilian Tensile Tests. *2*, 8. https://doi.org/10.5281/zenodo.3362989

Bu, C. M., Wen, K. J., Liu, S. H., Ogbonnaya, U., & Li, L. (2018). Development of bio-cemented constructional materials through microbial induced calcite precipitation. *Materials and Structures*, *51*(1), Article 30. https://doi.org/10.1617/s11527-018-1157-4

Cacciari, P. P., & Futai, M. M. (2018). Assessing the tensile strength of rocks and geological discontinuities via pull-off tests. *International Journal of Rock Mechanics and Mining Sciences*, *105*, 44-52. https://doi.org/10.1016/j.ijrmms.2018.03.011

Chen, C. S., & Hsu, S. C. (2001). Measurement of indirect tensile strength of anisotropic rocks by the ring test. *Rock Mechanics and Rock Engineering*, *34*(4), 293-321. https://doi.org/10.1007/s006030170003

Cheng, L., Kobayashi, T., & Shahin, M. A. (2020). Microbially induced calcite precipitation for production of "bio-bricks" treated at partial saturation condition. *Construction and Building Materials*, *231*, Article 117095. https://doi.org/10.1016/j.conbuildmat.2019.117095

Cheng, L., Shahin, M. A., & Mujah, D. (2017). Influence of Key Environmental Conditions on Microbially Induced Cementation for Soil Stabilization. *Journal of Geotechnical and Geoenvironmental Engineering*, *143*(1), Article 0001586. https://doi.org/10.1061/(asce)gt.1943-5606.0001586

Cui, M. J., Zheng, J. J., Zhang, R. J., Lai, H. J., & Zhang, J. (2017). Influence of cementation level on the strength behaviour of bio-cemented sand. *Acta Geotechnica*, *12*(5), 971-986. https://doi.org/10.1007/s11440-017-0574-9

Cunningham, A. B., Class, H., Ebigbo, A., Gerlach, R., Phillips, A. J., & Hommel, J. (2019). Field-scale modeling of microbially induced calcite precipitation. *Computational Geosciences*, *23*(2), 399-414. https://doi.org/10.1007/s10596-018-9797-6

Cunningham, A. B., Phillips, A. J., Troyer, E., Lauchnor, E., Hiebert, R., Gerlach, R., & Spangler, L. (2014, Oct 05-09). Wellbore leakage mitigation using engineered biomineralization.*Energy Procedia* [12th international conference on greenhouse gas control technologies, ghgt-12]. 12th International Conference on Greenhouse Gas Control Technologies (GHGT), Austin, TX.

Cunningham, A. R., Gerlach, R., Philipps, A., Lauchnor, E., Rothman, A., Hiebert, R., Busch, A., Lomans, B., & Spangler, L. (2015). Assessing potential for biomineralization sealing in fractured shale at the Mont Terri underground research facility, Switzerland. In (pp. 887-903).

Cuthbert, M. O., McMillan, L. A., Handley-Sidhu, S., Riley, M. S., Tobler, D. J., & Phoenix, V. R. (2013). A Field and Modeling Study of Fractured Rock Permeability Reduction Using Microbially Induced Calcite Precipitation. *Environmental Science & Technology*, *47*(23), 13637-13643. https://doi.org/10.1021/es402601g

Dowling, N. E., Kral, M. V., & Kampe, S. L. (2019). *Mechanical Behavior of Materials: Engineering Methods for Deformation, Fracture, and Fatigue*. Pearson Education, Incorporated.

Efimov, V. P. (2021). Brazilian Tensile Strength Testing. *Journal of Mining Science*, *57*(6), 922-932. https://doi.org/10.1134/S1062739121060053

Feder, M. J., Akyel, A., Morasko, V. J., Gerlach, R., & Phillips, A. J. (2021). Temperature-dependent inactivation and catalysis rates of plant-based ureases for engineered biomineralization. *Engineering Reports*, *3*(2), Article e12299. https://doi.org/10.1002/eng2.12299

Ferrill, D. A., Morris, A. P., Hennings, P. H., & Haddad, D. E. (2014). Faulting and fracturing in shale and self-sourced reservoirs: Introduction. *Aapg Bulletin*, *98*(11), 2161-2164. https://doi.org/10.1306/intro073014

Gale, J. F. W., Laubach, S. E., Olson, J. E., Eichhubl, P., & Fall, A. (2014). Natural fractures in shale: A review and new observations. *Aapg Bulletin*, *98*(11), 2165-2216. https://doi.org/10.1306/08121413151

Gao, Q., Tao, J. L., Hu, J. Y., & Yu, X. (2015). Laboratory study on the mechanical behaviors of an anisotropic shale rock. *Journal of Rock Mechanics and Geotechnical Engineering*, *7*(2), 213-219. https://doi.org/10.1016/j.jrmge.2015.03.003

Genedy, M., Kandil, U. F., Matteo, E. N., Stormont, J., & Taha, M. M. R. (2017). A new polymer nanocomposite repair material for restoring wellboreseal integrity. *International Journal of Greenhouse Gas Control*, *58*, 290-298. https://doi.org/10.1016/j.ijggc.2016.10.006

Genedy, M., Matteo, E. N., Stenko, M., Stormont, J. C., & Taha, M. R. (2019). Nanomodified Methyl Methacrylate Polymer for Sealing of Microscale Defects in Wellbore Systems. *Journal of Materials in Civil Engineering*, *31*(7), Article 04019118. https://doi.org/10.1061/(asce)mt.1943-5533.0002754

Hajiabadi, S. H., Khalifeh, M., van Noort, R., & Moreira, P. (2023). Review on Geopolymers as Wellbore Sealants: State of the Art Optimization for CO2 Exposure and Perspectives. *Acs Omega*, *8*(26), 23320-23345. https://doi.org/10.1021/acsomega.3c01777

Halder, B. K., Roy, D., Tandon, V., Ramana, C. V., & Tarquin, A. J. (2014). Use of Mutated Micro-Organism to Produce Sustainable Mortar. *Aci Materials Journal*, *111*(5), 511-519. <Go to ISI>://WOS:000341740500005

Hashiba, K., Okada, T., Tani, K., Shirasagi, S., Hayano, K., Nakamura, T., Oikawa, Y., Ono, M., Shimamoto, K., Yamada, S., Wakabayashi, N., Namikawa, T., & Nishikane, Y. (2017). Literature Survey and Experimental Study on the Direct Tension Test on Rocks. *Geotechnical Testing Journal*, *40*(2). https://doi.org/10.1520/gtj20160201

He, J. M., & Afolagboye, L. O. (2018). Influence of layer orientation and interlayer bonding force on the mechanical behavior of shale under Brazilian test conditions. *Acta Mechanica Sinica*, *34*(2), 349-358. https://doi.org/10.1007/s10409-017-0666-7

Hiebert, R. (2019). *Phase 1 SBIR Final Report: Permeability control for enhanced oil and gas recovery in unconventional reservoirs using advanced mineral precipitation technologies*.

Holt, R. M., Fjaer, E., Stenebraten, J. F., & Nes, O. M. (2015). Brittleness of shales: Relevance to borehole collapse and hydraulic fracturing. *Journal of Petroleum Science and Engineering*, *131*, 200-209. https://doi.org/10.1016/j.petrol.2015.04.006

Hou, B., Zeng, Y. J., Fan, M., & Li, D. D. (2018). Brittleness Evaluation of Shale Based on the Brazilian Splitting Test. *Geofluids*, Article Unsp 3602852. https://doi.org/10.1155/2018/3602852

Iferobia, C. C., Ahmad, M., & Ali, I. (2022). Experimental Investigation of Shale Tensile Failure under Thermally Conditioned Linear Fracturing Fluid (LFF) System and Reservoir Temperature Controlled Conditions. *Polymers (Basel)*, *14*(12). https://doi.org/10.3390/polym14122417

Illeová, V., Polakovic, M., Stefuca, V., Acai, P., & Juma, M. (2003). Experimental modelling of thermal inactivation of urease [Article]. *Journal of Biotechnology*, *105*(3), 235-243. https://doi.org/10.1016/j.jbiotec.2003.07.005

Illeova, V., Sefcik, J., & Polakovic, M. (2020). Thermal inactivation of jack bean urease [Article]. *International Journal of Biological Macromolecules*, *151*, 1084-1090. https://doi.org/10.1016/j.ijbiomac.2019.10.150

Jafariesfad, N., Sangesland, S., Gawel, K., & Torsaeter, M. (2020). New Materials and Technologies for Life-Lasting Cement Sheath: A Review of Recent Advances. *Spe Drilling & Completion*, *35*(2), 262-278. <Go to ISI>://WOS:000576605800010

Kim, G., Kim, J., & Youn, H. (2018). Effect of Temperature, pH, and Reaction Duration on Microbially Induced Calcite Precipitation. *Applied Sciences-Basel*, *8*(8), Article 1277. https://doi.org/10.3390/app8081277

Kirkland, C. M., Akyel, A., Hiebert, R., McCloskey, J., Kirksey, J., Cunningham, A. B., Gerlach, R., Spangler, L., & Phillips, A. J. (2021). Ureolysis-induced calcium carbonate precipitation (UICP) in the presence of CO2-affected brine: A field demonstration. *International Journal of Greenhouse Gas Control*, *109*, Article 103391. https://doi.org/10.1016/j.ijggc.2021.103391

Kirkland, C. M., Thane, A., Hiebert, R., Hyatt, R., Kirksey, J., Cunningham, A. B., Gerlach, R., Spangler, L., & Phillips, A. J. (2020). Addressing wellbore integrity and thief zone permeability using microbially-induced calcium carbonate precipitation (MICP): A field demonstration. *Journal of Petroleum Science and Engineering*, *190*, Article 107060. https://doi.org/10.1016/j.petrol.2020.107060

Krajewska, B. (2009). Ureases I. Functional, catalytic and kinetic properties: A review. *Journal of Molecular Catalysis B-Enzymatic*, *59*(1-3), 9-21. https://doi.org/10.1016/j.molcatb.2009.01.003

Krajewska, B. (2018). Urease-aided calcium carbonate mineralization for engineering applications: A review. *Journal of Advanced Research*, *13*, 59-67. https://doi.org/10.1016/j.jare.2017.10.009

Li, C. B., Zou, B. B., Zhou, H. W., & Wang, J. (2021). Experimental investigation on failure behaviors and mechanism of an anisotropic shale in direct tension. *Geomechanics and Geophysics for Geo-Energy and Geo-Resources*, *7*(4), Article 98. https://doi.org/10.1007/s40948-021-00294-x

Li, D. Y., & Wong, L. N. Y. (2013). The Brazilian Disc Test for Rock Mechanics Applications: Review and New Insights. *Rock Mechanics and Rock Engineering*, *46*(2), 269-287. https://doi.org/10.1007/s00603-012-0257-7

Li, H., Lai, B., Liu, H. H., Zhang, J., & Georgi, D. (2017). Experimental Investigation on Brazilian Tensile Strength of Organic-Rich Gas Shale. *Spe Journal*, *22*(1), 148-161. https://doi.org/10.2118/177644-pa

Liao, Z. Y., Zhu, J. B., & Tang, B. C. A. (2019). Numerical investigation of rock tensile strength determined by direct tension, Brazilian and three-point bending tests. *International Journal of Rock Mechanics and Mining Sciences*, *115*, 21-32. https://doi.org/10.1016/j.ijrmms.2019.01.007

Mellor, M., & Hawkes, I. (1971). Measurement of tensile strength by diametral compression of discs and annuli. *Engineering Geology*, *5*(3), 173-225. https://doi.org/https://doi.org/10.1016/0013-7952(71)90001-9

Mews, K. S., Alhubail, M. M., & Barati, R. G. (2019). A Review of Brittleness Index Correlations for Unconventional Tight and Ultra-Tight Reservoirs. *Geosciences*, *9*(7), Article 319. https://doi.org/10.3390/geosciences9070319

Mobley, H. L. T., & Hausinger, R. P. (1989). MICROBIAL UREASES - SIGNIFICANCE, REGULATION, AND MOLECULAR CHARACTERIZATION. *Microbiological Reviews*, *53*(1), 85-108. https://doi.org/10.1128/mmbr.53.1.85-108.1989

Mokhtari, M., Honarpour, M. M., Tutuncu, A. N., & Boitnott, G. N. (2014). Acoustical and Geomechanical Characterization of Eagle Ford Shale - Anisotropy, Heterogeneity and Measurement Scale. SPE Annual Technical Conference and Exhibition,

Montoya, B. M., & DeJong, J. T. (2015). Stress-Strain Behavior of Sands Cemented by Microbially Induced Calcite Precipitation. *Journal of Geotechnical and Geoenvironmental Engineering*, *141*(6), Article 04015019. https://doi.org/10.1061/(asce)gt.1943-5606.0001302

Myers, T. (2012). Potential Contaminant Pathways from Hydraulically Fractured Shale to Aquifers. *Groundwater*, *50*(6), 872-882. https://doi.org/https://doi.org/10.1111/j.1745-6584.2012.00933.x

Ng, W., Lee, M., & Hii, S. (2012). An Overview of the Factors Affecting Microbial-Induced Calcite Precipitation and its Potential Application in Soil Improvement. *World Academy of Science, Engineering and Technology, Open Science Index 62, International Journal of Civil and Environmental Engineering*, *6*(2), 188 - 194.

Park, S. S., Choi, S. G., & Nam, I. H. (2014). Effect of Plant-Induced Calcite Precipitation on the Strength of Sand. *Journal of Materials in Civil Engineering*, *26*(8), Article 06014017. https://doi.org/10.1061/(asce)mt.1943-5533.0001029

Peters, K. E., Xia, X., Pomerantz, A. E., & Mullins, O. C. (2016). Chapter 3 - Geochemistry Applied to Evaluation of Unconventional Resources. In Y. Z. Ma & S. A. Holditch (Eds.),

Unconventional Oil and Gas Resources Handbook (pp. 71-126). Gulf Professional Publishing. https://doi.org/https://doi.org/10.1016/B978-0-12-802238-2.00003-1

Phillips, A. J., Cunningham, A. B., Gerlach, R., Hiebert, R., Hwang, C. C., Lomans, B. P., Westrich, J., Mantilla, C., Kirksey, J., Esposito, R., & Spangler, L. (2016). Fracture Sealing with Microbially-Induced Calcium Carbonate Precipitation: A Field Study. *Environmental Science & Technology*, *50*(7), 4111-4117. https://doi.org/10.1021/acs.est.5b05559

Phillips, A. J., Gerlach, R., Lauchnor, E., Mitchell, A. C., Cunningham, A. B., & Spangler, L. (2013). Engineered applications of ureolytic biomineralization: a review. *Biofouling*, *29*(6), 715-733. https://doi.org/10.1080/08927014.2013.796550

Phillips, A. J., Lauchnor, E., Eldring, J., Esposito, R., Mitchell, A. C., Gerlach, R., Cunningham, A. B., & Spangler, L. H. (2013). Potential CO2 Leakage Reduction through Biofilm-Induced Calcium Carbonate Precipitation. *Environmental Science & Technology*, *47*(1), 142-149. https://doi.org/10.1021/es301294q

Phillips, A. J., Troyer, E., Hiebert, R., Kirkland, C., Gerlach, R., Cunningham, A. B., Spangler, L., Kirksey, J., Rowe, W., & Esposito, R. (2018). Enhancing wellbore cement integrity with microbially induced calcite precipitation (MICP): A field scale demonstration. *Journal of Petroleum Science and Engineering*, *171*, 1141-1148. https://doi.org/10.1016/j.petrol.2018.08.012

RCoreTeam. (2022). *R: A language and environment for statistical computing*. R Foundation for Statistical Computing, Vienna, Austria. https://www.R-project.org/

Rodriguez, J., Heo, J., & Kim, K. H. (2020). The Impact of Hydraulic Fracturing on Groundwater Quality in the Permian Basin, West Texas, USA. *Water*, *12*(3), 796. https://www.mdpi.com/2073-4441/12/3/796

Sahrawat, K. L. (1984). Effects of temperature and moisture on urease activity in semi-arid tropical soils. *Plant and Soil*, *78*(3), 401-408. https://doi.org/10.1007/BF02450373

Scotchman, I. (2016). Shale gas and fracking: Exploration for unconventional hydrocarbons. *Proceedings of the Geologists' Association*, *127*. https://doi.org/10.1016/j.pgeola.2016.09.001

Simpson, N. D. J., Stroisz, A., Bauer, A., Vervoort, A., & Holt, R. M. (2014). Failure Mechanics Of Anisotropic Shale During Brazilian Tests. 48th U.S. Rock Mechanics/Geomechanics Symposium,

Skorupa, D. J., Akyel, A., Fields, M. W., & Gerlach, R. (2019). Facultative and anaerobic consortia of haloalkaliphilic ureolytic micro-organisms capable of precipitating calcium carbonate. *Journal of Applied Microbiology*, *127*(5), 1479-1489. https://doi.org/10.1111/jam.14384

Stocks-Fischer, S., Galinat, J. K., & Bang, S. S. (1999). Microbiological precipitation of CaCO3. *Soil Biology & Biochemistry*, *31*(11), 1563-1571. https://doi.org/10.1016/s0038-0717(99)00082-6

Todorovic, J., Raphaug, M., Lindeberg, E., Vralstad, T., & Buddensiek, M. L. (2015, Jun 16-18). Remediation of Leakage through Annular Cement Using a Polymer Resin: a Laboratory Study.*Energy Procedia* [8th trondheim conference on co2 capture, transport and storage]. 8th Trondheim Conference on CO2 Capture, Transport and Storage (TCCS), Trondheim, NORWAY.

U.S.E.I.A. (2016). *Shale gas and oil plays, Lower 48 States*. U.S. Energy Information Administration. https://www.eia.gov/maps/maps.htm

Vengosh, A., Jackson, R. B., Warner, N., Darrah, T. H., & Kondash, A. (2014). A Critical Review of the Risks to Water Resources from Unconventional Shale Gas Development and Hydraulic Fracturing in the United States. *Environmental Science & Technology*, *48*(15), 8334-8348. https://doi.org/10.1021/es405118y

Vishal, V., Rizwan, M., Mahanta, B., Pradhan, S. P., & Singh, T. N. (2022). Temperature effect on the mechanical behavior of shale: Implication for shale gas production. *Geosystems and Geoenvironment*, *1*(4), 100078. https://doi.org/https://doi.org/10.1016/j.geogeo.2022.100078

Vizini, V. O. S., Cacciari, P. P., & Futai, M. M. (2020). Numerical Assessment of Factors Influencing the Tensile Strength of Rocks via Pull-Off Test. *International Journal of Geomechanics*, *20*(7), Article 04020075. https://doi.org/10.1061/(asce)gm.1943-5622.0001714

Wang, C. H., Gao, G. Y., Jia, Q., & Wang, C. Q. (2020). Investigation of optimum sample shape for the Luong core tension test. *Bulletin of Engineering Geology and the Environment*, *79*(2), 831-844. https://doi.org/10.1007/s10064-019-01607-x

Wang, J., Xie, L. Z., Xie, H. P., Ren, L., He, B., Li, C. B., Yang, Z. P., & Gao, C. (2016). Effect of layer orientation on acoustic emission characteristics of anisotropic shale in Brazilian tests. *Journal of Natural Gas Science and Engineering*, *36*, 1120-1129. https://doi.org/10.1016/j.jngse.2016.03.046

Wang, J. Y., Soens, H., Verstraete, W., & De Belie, N. (2014). Self-healing concrete by use of microencapsulated bacterial spores. *Cement and Concrete Research*, *56*, 139-152. https://doi.org/https://doi.org/10.1016/j.cemconres.2013.11.009

Wang, Q., Chen, X., Jha, A. N., & Rogers, H. (2014). Natural gas from shale formation – The evolution, evidences and challenges of shale gas revolution in United States. *Renewable and Sustainable Energy Reviews*, *30*, 1-28. https://doi.org/https://doi.org/10.1016/j.rser.2013.08.065

Wang, Y., Wang, Y., Soga, K., DeJong, J. T., & Kabla, A. J. (2023). Microscale investigations of temperature-dependent microbially induced carbonate precipitation (MICP) in the temperature range 4–50 °C. *Acta Geotechnica*, *18*(4), 2239-2261. https://doi.org/10.1007/s11440-022-01664-9

Willett, M. R., Bedey, K., Dobeck, L., Crandall, D., Moore, J., Rutqvist, J., Cunningham, A. B., Seymour, J. D., Eldring, J., Phillips, A., & Kirkland, C. M. (2023). *Using Low-Field Nuclear Magnetic Resonance and Computed Tomography Imaging to Explore Potential of Ureolysis-Induced Calcium Carbonate Precipitation Treatment to Seal Fractures in Shale* In preparation for the conference preceeding of the 57th US Rock Mechanics/Geomechanics Symposium, Atlanta, GA.

Willett, M. R., Seymour, J. D., Bedey, K., Kirkland, C. M., Phillips, A. J., Cunningham, A. B., Dobeck, L., Crandall, D., & Rutqvist, J. (2023). Using Low-Field Nuclear Magnetic Resonance and X-Ray Computed Microtomography Imaging to Explore Potential of Microbially-Induced Calcium Carbonate Precipitation Treatment to Seal Shale Fractures. 57th U.S. Rock Mechanics/Geomechanics Symposium,

Xiao, Y., Wang, Y., Desai, C. S., Jiang, X., & Liu, H. L. (2019). Strength and Deformation Responses of Biocemented Sands Using a Temperature-Controlled Method. *International Journal of Geomechanics*, *19*(11), Article 04019120. https://doi.org/10.1061/(asce)gm.1943-5622.0001497

Yasuhara, H., Neupane, D., Hayashi, K., & Okamura, M. (2012). Experiments and predictions of physical properties of sand cemented by enzymatically-induced carbonate precipitation. *Soils and Foundations*, *52*(3), 539-549. https://doi.org/10.1016/j.sandf.2012.05.011

APPENDIX

STATISTICAL METHODS FOR CHAPTER 2 DATA

R version 4.2.1 (R Core Team 2022) was used to analyze data in Chapter 2. A two-sample t-test investigated the difference in average tensile strength values for Eagle Ford and Wolfcamp shale cores tested at room temperature and 60°C. Two separate two-sample t-tests were run to investigate the effect temperature had on Eagle Ford and Wolfcamp cores independently, ultimately to determine if there was a statistical difference between cores tested at room temperature versus cores tested at 60°C. Another two-sample t-test compared the averages of all Eagle Ford samples versus all Wolfcamp samples to determine if there was a statistical difference in tensile strength of one shale type compared to the other.